

Section 3: Chapter 9

MALDI-TOF MS Methods for Evaluation of *in vitro* Aminoacyl tRNA Production

The unnatural amino acids experiments described in this thesis require the *in vitro* production of an aminoacyl suppressor tRNA (aa-tRNA_{CUA}).¹ This is used to deliver our unnatural amino acid at the site of a mutagenically introduced stop codon. The aa-tRNA_{CUA} are made by ligating a chemically synthesized aminoacyl dCA dinucleotide to the 3' end of a transcribed 74mer tRNA_{CUA} (tRNA_{CUA}^{-CA}). Prior to this work, there was no simple technique for evaluating the aminoacylation state of the tRNA before using it in translation. Available methods relied on gel electrophoresis, which infers mass from electrophoretic mobility. Radiolabelling could be used to ascertain aminoacylation information,² but this was impractical for the “everyday” production of tRNA_{CUA}s for suppression. Aminoacyl tRNAs can be observed on acid/urea gels, but very long running times are required.^{3, 4}

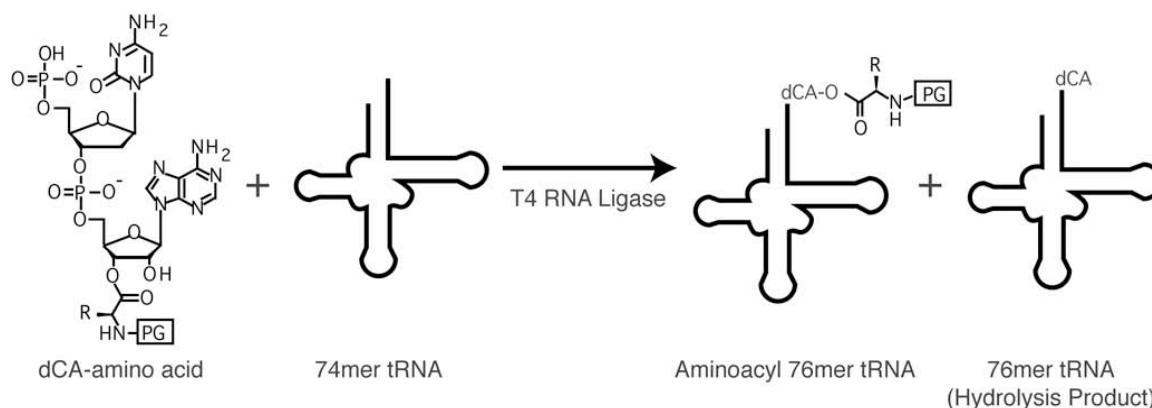


Figure 1. T4 RNA Ligase Reaction. The synthesized aminoacyl dinucleotide dCA is ligated to transcribed 74mer tRNA with T4 RNA ligase to give aminoacyl 76mer tRNA. Hydrolysis of the 3' ester bond gives 76mer tRNA. PG indicates that α -amine is protected as an amide functionality.

We found that matrix-assisted laser desorption/ionization time-of-flight mass spectrometry (MALDI-TOF MS)^{5, 6} provides a simple and quick way of evaluating the products of the ligase reaction. It is also much more precise, enabling one to easily distinguish tRNA species down to the single nucleotide level, and to verify the identity of the amino acid. The use of MALDI MS with tRNA was not new,^{7, 8} but we demonstrated its application to a novel problem. Here, MALDI-TOF MS is used to monitor the production of aa-tRNA_{CUA} by following the disappearance of 74mer starting material and the appearance of the desired aa-76mer and the 76mer hydrolysis product.

The suppressor tRNA is produced through a combination of chemical and biological steps. The amino acid to be delivered is made as an α -amino-protected cyanomethyl ester which is coupled to chemically synthesized pdCpA. The suppressor tRNA is transcribed from linearized cDNA as a 74mer lacking its 3' CA. This transcript is ligated to the 5' phospho-dCA-amino acid (dCA-aa) with T4 RNA ligase (Fig. 1).⁹ The amino acid is then deprotected just prior to use in translation with an mRNA bearing the stop codon to which the tRNA_{CUA} will deliver its amino acid.

Traditionally, the reactions in the chemical steps have been monitored by thin-layer chromatography and high performance liquid chromatography, and the ligation step by gel electrophoresis. (Fig. 2) One can easily differentiate unligated 74mer from 76mer produced either through transcription (76/77mer, some untemplated 77mer, see Materials and Methods) or ligation (dCA 76mer). One can also observe the aminoacyl tRNA_{CUA}s Ala-76mer, Trp-76mer, and 5-cyano-tryptophan-76mer (5-CN-Trp-76mer). However, there are substantial amounts of the 76mer hydrolysis product present. Even under acid/urea gel conditions, (See Materials and Methods) some of the aa-76mer may have hydrolyzed in the 36 hour process of running the gel. This seems to be the case; mass spectra of the same tRNA samples (Fig. 3) shows them to be relatively free of 76mer hydrolysis product. In contrast, the gel shows nearly equivalent amounts of aa-76mer and 76mer hydrolysis product. This illustrates one of the several advantages of MALDI MS over gel electrophoresis as an analytical tool for our problem. A successful application of MALDI MS takes less time to run, uses less tRNA material, is more precise, and most importantly, provides aminoacylation information that cannot be obtained through gel techniques.

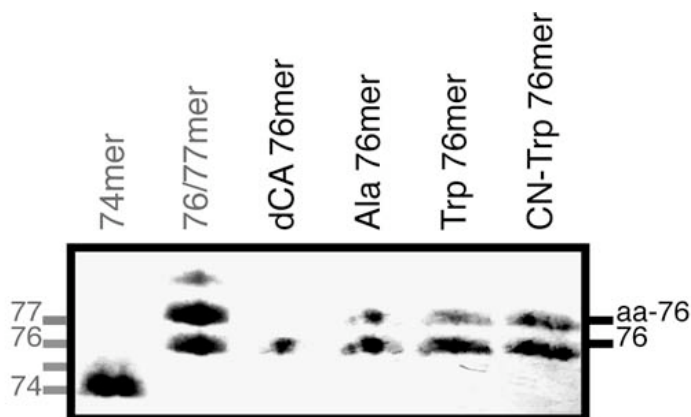


Figure 2. Gel Separation of tRNA Species. 20 % polyacrylamide acid/urea gel showing single base resolution. 74mer and 76/77mer (in gray) are transcribed from cDNA. Corresponding markers are shown in gray at left. All others (in black) are produced through T4 RNA ligase reaction of either dCA or dCA-aa with transcribed 74mer. One can observe both the aa-76mer and 76mer hydrolysis product, marked at right in black.

In order to identify a suitable matrix for analysis of the tRNAs, a variety of matrices were tested with 74mer transcript. These included 3-hydroxypicolinic acid (3-HPA),¹⁰ 6-aza-2-thiothymine,⁷ 2,4,6-trihydroxyacetophenone,¹¹ and anthranilic/nicotinic acid (AA/NA) mixtures.¹² Among these, only 3-HPA and AA/NA (2.7mg AA and 1.2 mg NA in 50 μ l CH₃CN and 60 μ l 50 mM diammonium citrate (DAC)) provided acceptable 74mer signal intensity. 3-HPA was chosen because it resulted in superior mass resolution and intensity. Ammonium-loaded cation-exchange beads improved signal intensities dramatically for the 74mer tRNA. More importantly, a ten minute treatment with the NH₄⁺-loaded beads (See Materials and Methods) was found to be essential to observing the aminoacyl tRNAs. The H⁺ and N(Bu)₄⁺ forms of the beads were found to produce inferior results.

The final, optimized matrix sample preparation routinely resolves 74mer transcripts from 76mer and aa-76mer tRNAs (Fig. 3). Figure 3 depicts the same tRNA samples that were loaded onto the gel shown in Figure 2: transcribed 74mer, transcribed 76/77mer, ligated dCA 76mer, and Ala, Trp, and CN-Trp aa-76mers. One can see that hydrolysis of the amino acid has been minimal; the 76mer observed on the gel must have been produced in the process of running the gel.

The aa-76mer peaks are noticeably broader than the 74mer or even dCA 76mer peak. It is tempting to attribute the change in resolution to contaminants, as it seems surprising that aminoacylation, a relatively small change on the scale of a tRNA, would cause such a dramatic change in its behavior in the MALDI MS. The repeated phenol/chloroform/isoamyl alcohol extractions described in Materials and Methods were crucial to attaining the level of resolution shown in Figure 3. However, further extraction does not improve the aa-76mer signal, so it seems that residual ligation reagents are not limiting the resolution. This question could be addressed by gel purifying the aa-tRNAs prior to analyzing them, but this experiment has not been performed. The loss of resolution observed may be attributable to increased matrix-adduct formation by the aa-76mer relative to the dCA-76mer.

The resolution of aa-76mer from 76mer is aided by the fact that the amino acid is protected on its α -amine with a nitroveratryloxycarbonyl group (NVOC, 241 Da), increasing the mass shift. The inherent error of our system is about 0.1 %. (See Materials and Methods) This precludes resolving an alanyl tRNA from a glycyl tRNA, but one can still gain ample information about most ligation reactions.

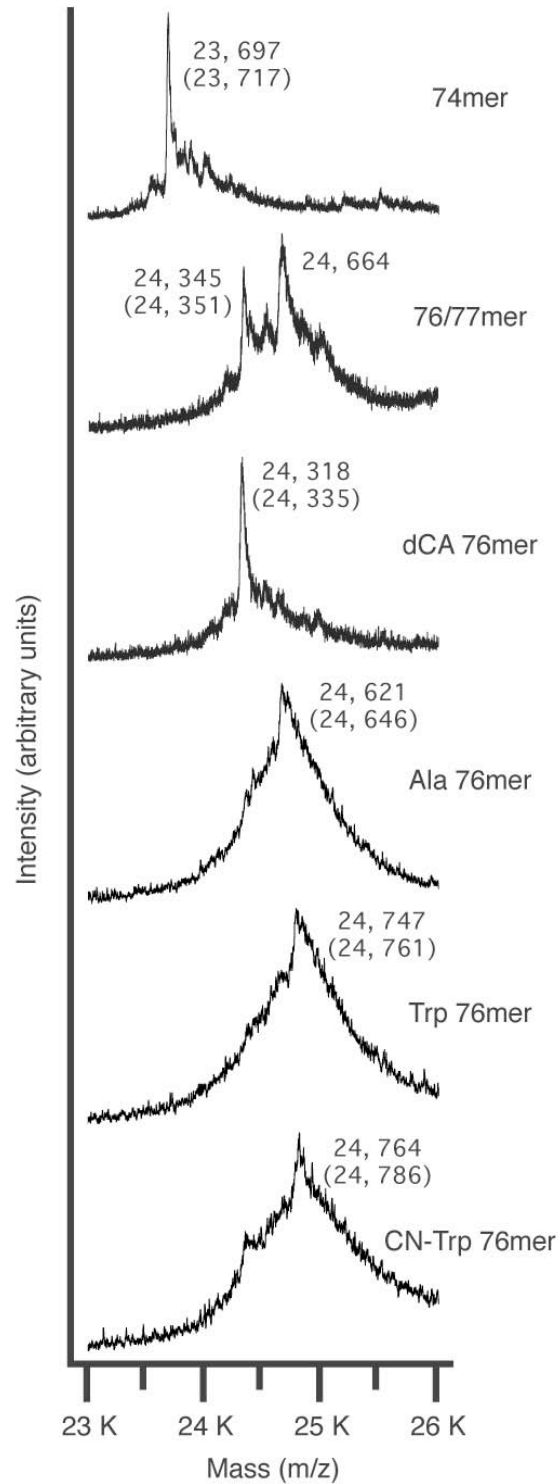


Figure 3. MALDI Mass Spectra of Various tRNA Species. The tRNA species shown are the same as those shown in the gel in Figure 2. Comparing the 74mer to the dCA-76mer shows that the addition of the dinucleotide can be clearly observed. The further increase in mass attributable to the amino acid is also clear in the Ala-76mer, Trp-76mer, and CN-Trp-76mer spectra. A small amount of 76mer hydrolysis product is apparent in the spectra of the aminoacyl tRNA. Observed masses (average of 5 spectra) are shown, with expected masses given in parentheses. The MS data confirms gel data indicating the presence of untemplated 77mer in the transcribed 76mer.

It should be noted that the masses we observe are consistent with tRNAs lacking the 5' phosphorylation expected of a T7 RNA polymerase product. The 5' phosphate bond has been identified as one of the most labile RNA bonds in MALDI MS conditions, though RNAs are known to be generally stable in MALDI-TOF MS.^{6, 13} While this may be cause for concern that any deaminoacylation observed is also a result of the MALDI process, the fact that we observe pure aa-76mer should assuage this concern.

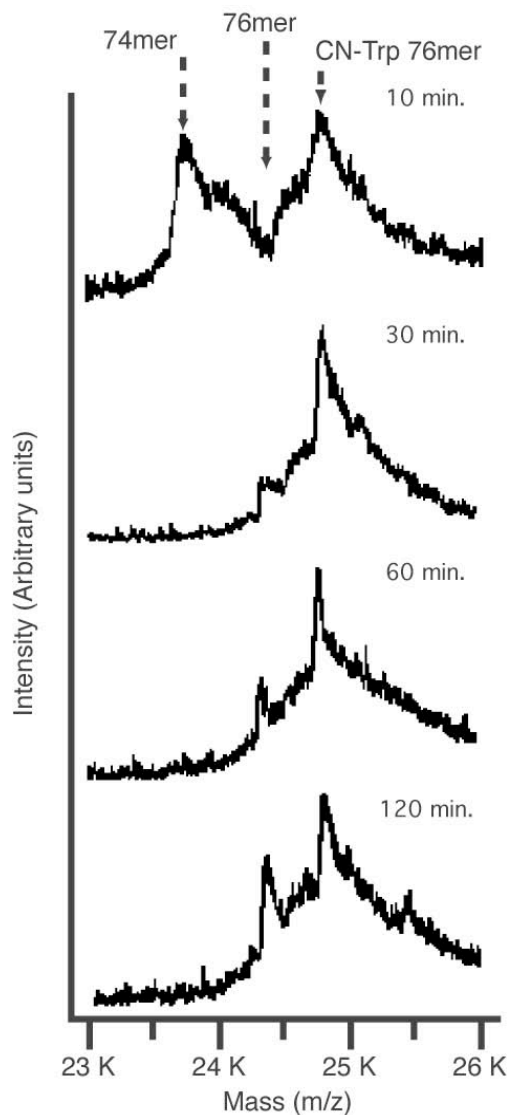


Figure 4. T4 RNA Ligase Reaction Efficiency. MALDI mass spectra of aliquots of the ligation of 5-CN-Trp-dCA taken after various reaction times. At 10 minutes, starting material (74mer), hydrolysis product (dCA 76mer) and desired product (CN-Trp 76mer) are clearly seen. The reaction is complete after 20 - 30 minutes, and longer reaction times lead only to increased hydrolysis (giving dCA 76mer).

In a valuable application of this methodology, monitoring the T4 ligation reaction by MALDI-TOF MS has shown that the usual two hour incubation time¹⁴ leads to substantial hydrolysis of the amino acid (Fig. 4). In fact, the reaction is largely complete after 20

minutes, and incubation times longer than 30 minutes are unnecessary. This has held true for a wide variety of both natural and unnatural amino acids, including Ala, Trp, CN-Trp, and two positively charged tyrosine derivatives. While one can get a clear impression of the degree of hydrolysis from mass spectra like those in Figure 4, it is not possible to quantitate the relative amounts of 76mer and aa-76mer. The decrease in resolution (see above) for the aa-tRNAs indicates that they ionize differently than non-aminoacyl tRNAs making it unreasonable to compare peak intensities.

One major improvement was made subsequent to the initial development of these protocols. Size-exclusion chromatography was used to purify the aa-tRNA_{CUA} away from unligated dCA-aa. This led to much sharper peaks in the MALDI spectra and greater reproducibility of the data. (Fig. 5) In the original process, peaks would often be extremely broad or the tRNAs would sometimes not “fly” at all in the mass spectrometer.

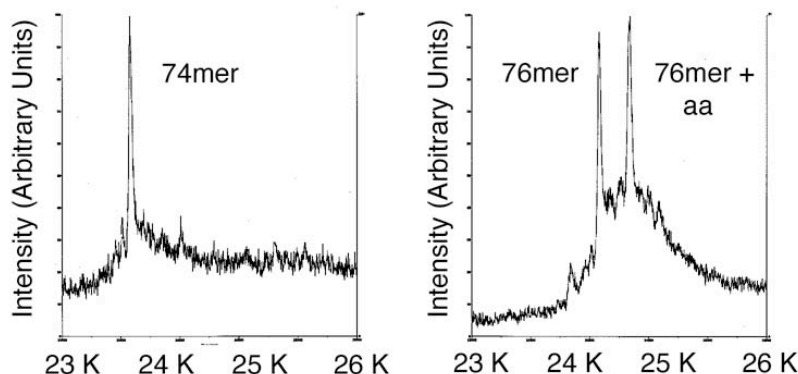


Figure 5. MS of High Purity tRNA Species. tRNA species isolated with improved column protocol.

MALDI MS can also be used to observe the photocleavage of the NVOC protecting group from the aminoacyl tRNA_{CUA}s. An example of monitoring photodeprotection is shown in Chapter 7, Figure 13. Removing the NVOC protecting group prior to using the tRNA in translation is essential; the α -amine must be exposed in order for it to be incorporated into the peptide backbone. Time course studies similar to those performed for the ligation reaction can be used to determine optimal photodeprotection conditions. This again, is information inaccessible through gel electrophoresis.

MALDI MS has proven useful in evaluating the dCA ligation reaction as well as in examining the deprotection of the α -amines of the aa-76mers. Not only is the MALDI analysis faster and more material-efficient than gel electrophoresis, it can provide information about the aminoacylation state of the tRNA unobtainable through gels. We have applied the assay to a relatively specific problem, but the techniques should prove useful to those interested in tRNA aminoacylation, particularly those engineering synthetases.

Materials and Methods

Materials

The synthesis of the pdCpA dinucleotide and its 3' aminoacylation have been described previously, as have the syntheses of the protected natural and unnatural amino acids which are coupled to the dCA for ligation.^{14, 15} All water used in the enzymatic reactions below has been rendered RNase-free by treatment with diethylpyrocarbonate (Sigma-Aldrich, St. Louis, MO). The chemicals used in matrix preparation, α -cyano-4-hydroxycinnamic acid (α -CN), 3-hydroxypicolinic acid (3-HPA), picolinic acid (PA), diammonium citrate (DAC), and DOWEX 50WX8-200 100-200 mesh size ion exchange resin, were also purchased from Sigma. The DOWEX beads were exchanged overnight with 1 M NH_4OAc , collected on a frit, and washed twice with 1 M NH_4OAc . CHROMA SPIN-30 DEPC- H_2O columns were purchased from BD Biosciences (San Jose, CA).

Transcription of 74mer and 76mer tRNA_{CUA}

The transcription and ligations have been previously described; they were performed here with minor alterations.¹⁶ The tRNA used was THG73, *Tetrahymena thermophila* tRNA^{Gln}CUA having a G at position 73. This gene contains an upstream T7 RNA polymerase promoter and downstream restriction sites. *Fok I* digestion provided the 74mer template and *Bsa I* digestion gave the 76mer template. The *in vitro* transcription of linearized cDNA to produce THG73 74mer and 76mer tRNAs was performed with the Ambion T7-MEGAscript kit (Austin, TX). Transcripts were isolated with a 25:24:1 phenol/ CHCl_3 /isoamyl alcohol (PCI) extraction. The organic layer was reextracted with water and a 24:1 CHCl_3 /isoamyl alcohol (CI) was performed on the combined aqueous layers. The water layer was then mixed with an equal volume of isopropanol, precipitated overnight at -20°C , pelleted, dried, and redissolved in H_2O . The 76mer tRNA appears to contain a large amount of untemplated 77mer and will be referred to as 76/77mer. There is substantial precedent for the addition of untemplated nucleotides at both the 3' and 5' ends of T7 RNA polymerase transcription products.¹⁷

Ligation of dCA-aa to 74mer tRNA_{CUA} (tRNA_{CUA}^{-CA})

Prior to ligation, the 74mer tRNAs were heated to 90°C in a 6.7 mM HEPES (pH 7.5) solution and allowed to cool to 37°C . They were then incubated at 37°C in 40 μl of a ligation mixture containing 42 mM HEPES (pH 7.5), 10% dimethylsulfoxide (v/v), 4 mM dithiothreitol, 20 mM MgCl_2 , 0.2 mg/ml bovine serum albumin (Ambion), 150 μM ATP, 10 μM 74mer tRNA transcript, 300 μM protected dCA-aa, and 2,000 units/ml T4 RNA ligase (New England Biolabs, Beverly, MA). After incubation at 37°C for 10 to 120 minutes, the reaction mixtures were diluted to 100 μl by adding 8.3 μl 3.0 M NaOAc and 51.7 μl H_2O .

They were then extracted against an equal volume of PCI (pH adjusted to 4.5 with NaOAc). The organic layer was reextracted with 4.2 μ l 3.0 M NaOAc and 45.8 μ l H₂O. Aqueous layers were combined and extracted again with 150 μ l PCI. Two 150 μ l CI extractions were performed on the water layer. Finally, the water layer was mixed with 450 μ l EtOH and precipitated overnight at -20 °C. The sample was pelleted, dried, and resuspended in 1 mM NaOAc to 1.0 μ g/ μ l (DNA quantified by UV absorption at 260 nm).

MALDI Mass Spectrometry

All tRNAs were analyzed on a PerSeptive Biosystems (Framingham, MA) Voyager DE PRO MALDI-TOF mass spectrometer operating in linear and positive ion modes. For all experiments the accelerating voltage was held at + 25 kV, grid voltage at 92.5%, and guide wire at 0.15%; delay was 500 ns. The nitrogen laser power was set to the minimum level necessary to generate a reasonable signal (except in those experiments in which we attempted to degrade the tRNA). Generally, a two point external calibration was performed, using the M³⁺ (22, 144 Da) and M²⁺ (33,216 Da) peaks of bovine serum albumin (BSA) (PE Biosystems, Foster City, CA) in an α -CN matrix (saturated in 2:1 H₂O/CH₃CN). For tRNA analyses, the matrix solution consisted of 42 mg 3-HPA, 2 mg PA, and 2 mg DAC dissolved in 500 μ l 9:1 H₂O/CH₃CN. A 1.0 μ l aliquot of tRNA was exchanged with \sim 2 μ l ammonium-loaded cation-exchange beads for ten minutes prior to loading and mixed with 2.0 μ L matrix. 0.5 μ l of the resulting solution was spotted on the MALDI sample target and allowed to dry at room temperature. The mass accuracy with external calibration using BSA is estimated to be about 0.1%, or 25 Da for tRNAs of this size. Internal calibrations were performed to eliminate the possibility that mass accuracy was affected by the difference in crystal heights between the α -CN matrix used for calibration and the 3-HPA matrix used with the tRNAs. Apomyoglobin (16, 953 Da) or DNA 40 and 88mers (12, 111 and 27, 210 Da) were used as standards.

Gel Electrophoresis

4 μ g samples of various tRNA species were resolved on a 20 % polyacrylamide (19:1 acrylamide/bis) gel in TBE (10 X from BioRad, Hercules, CA), 7 M urea, and 0.1 M NaOAc (solution also used to pour gel). The 1.6 mm thick gel was run for 48 hours (1.25 times the amount of time required to run bromophenol blue dye off the gel) at 500 V and stained overnight with Stains-all (Sigma-Aldrich). Procedure adapted from acid/urea gel techniques used by Varshney *et al.*⁴

Column Purification

Before use, the CHROMA SPIN-30 DEPC-H₂O column was shaken by hand to ensure mixing of gel. It was then spun for 2 min. at 3000 rpm. in a benchtop centrifuge to

remove water from the column. The flow through was discarded and the spinning was repeated to ensure the dryness of the column. The tRNA solution (after ligation, PCI work up, precipitation, and redissolution) was applied to the center of the CHROMA SPIN column. It was important not to allow the solution to touch the sides of the column. The tRNA solution was then eluted from the CHROMA SPIN column by spinning for 5 min. at 3000 rpm. It could then be taken on to the MALDI MS process or to oocyte injection.

References

- (1) Cornish, V. W.; Mendel, D.; Schultz, P. G., *Angew. Chem. Int. Ed.* **1995**, 34, 621-633
Dougherty, D. A., *Curr. Opin. Chem. Biol.* **2000**, 4, 645-652.
- (2) Weygand-Durasevic, I.; Lenhard, D.; Filipic, S.; Soll, D., *J. Biol. Chem.* **1996**, 271, 2455-2461.
- (3) Kohrer, C.; Xie, L.; Kellerer, S.; Varshney, U.; Rajbhandary, U. L., *Proc. Natl. Acad. Sci. USA* **2001**, 98, 14310-14315 Wolfson, A. D.; Pleiss, J. A.; Uhlenbeck, O. C., *RNA* **1998**, 4, 1019-1023.
- (4) Varshney, U.; Lee, C. P.; Rajbhandary, U. L., *J. Biol. Chem.* **1991**, 266, 24712-24718.
- (5) Bakhtiar, R.; Nelson, R. W., *Biochem. Pharmacol.* **2000**, 59, 891-905 Bakhtiar, R.; Tse, F. L. S., *Mutagenesis* **2000**, 15, 415-430 Zenobi, R.; Knochenmuss, R., *Mass Spectrom. Rev.* **1998**, 17, 337-366.
- (6) Kirpekar, F.; Nordhoff, E.; Kristiansen, K.; Roepstorff, P.; Lezius, A.; Hahner, S.; Karas, M.; Hillenkamp, F., *Nucleic Acids Res.* **1994**, 22, 3866-3870.
- (7) Gruic-Sovulj, I.; Ludemann, H. C.; Hillenkamp, F.; Weygand-Durasevic, I.; Kucan, Z.; Peter-Katalinic, J., *J. Biol. Chem.* **1997**, 272, 32084-32091.
- (8) Rubelj, I.; Weygand-Durasevic, I.; Kucan, Z., *Eur. J. Biochem.* **1990**, 193, 783-788 Sochacka, E.; Czerwinska, G.; Guenther, R.; Cain, R.; Agris, P. F.; Malkiewicz, A., *Nucleosides Nucleotides Nucleic Acids* **2000**, 19, 515-531 Sovulj, I. G.; Weygand-Durasevic, I.; Kucan, Z., *Croat. Chem. Acta* **2001**, 74, 161-171 Wei, J.; Lee, C. S., *Anal. Chem.* **1997**, 69, 4899-4904.
- (9) Silber, R.; Malathi, V. G.; Hurwitz, J., *Proc. Natl. Acad. Sci. USA* **1972**, 69, 3009-3013 Uhlenbeck, O. C.; Gumpert, R. I., T4 RNA Ligase. In *The Enzymes.*; Boyer, P. D., Academic Press, Inc.: New York, NY, 1982; 31-58 Uhlenbeck, O. C., *Trends Biochem. Sci.* **1983**, 8, 94-96.
- (10) Kirpekar, F.; Douthwaite, S.; Roepstorff, P., *RNA* **2000**, 6, 296-306 Tolson, D. A.; Nicholson, N. H., *Nucleic Acids Res.* **1998**, 26, 446-451.
- (11) Patteson, K. G.; Rodicio, L. P.; Limbach, P. A., *Nucleic Acids Res.* **2001**, 29, 00.
- (12) Zhang, L. K.; Gross, M. L., *J. Am. Soc. Mass Spectrom.* **2000**, 11, 854-865.
- (13) Kirpekar, F.; Krogh, T. N., *Rapid Commun. Mass Spectrom.* **2001**, 15, 8-14 Knochenmuss, R.; Stortelder, A.; Breuker, K.; Zenobi, R., *J. Mass Spectrom.* **2000**, 35, 1237-1245 Nordhoff, E.; Cramer, R.; Karas, M.; Hillenkamp, F.; Kirpekar, F.; Kristiansen, K.; Roepstorff, P., *Nucleic Acids Res.* **1993**, 21, 3347-3357.
- (14) Nowak, M. W.; Gallivan, J. P.; Silverman, S. K.; Labarca, C. G.; Dougherty, D. A.; Lester, H. A., *Methods Enzymol.* ; 1998; 293, 504-529.
- (15) Ellman, J.; Mendel, D.; Anthonycahill, S.; Noren, C. J.; Schultz, P. G., *Methods Enzymol.* **1991**, 202, 301-336.
- (16) Saks, M. E.; Sampson, J. R.; Nowak, M. W.; Kearney, P. C.; Du, F.; Abelson, J. N.; Lester, H. A.; Dougherty, D. A., *J. Biol. Chem.* **1996**, 271, 23169-23175.
- (17) Helm, M.; Brule, H.; Giege, R.; Florentz, C., *RNA* **1999**, 5, 618-621 Kao, C.; Zheng, M.; Rudisser, S., *RNA* **1999**, 5, 1268-1272 Milligan, J. F.; Groebe, D. R.; Witherell, G. W.; Uhlenbeck, O. C., *Nucleic Acids Res.* **1987**, 15, 8783-8798 Pleiss, J. A.; Derrick, M. L.; Uhlenbeck, O. C., *RNA* **1998**, 4, 1313-1317.

Section 3: Chapter 10

Preparation of Photoactivatable Agonists for Studies of Fluorescently Labeled Nicotinic Acetylcholine Receptors

Despite the exquisite sensitivity of electrophysiology, it is an imperfect technique for studying the gating process of ion channels. A current signal is only observed once the channel has undergone a sufficiently large conformational change to open the pore to permit ion flow. This state is necessarily near the end of the gating process. To understand the process by which agonist binding induces gating, we must be able to measure events in the gating process that occur “upstream” of channel opening. We chose to do this by attaching a fluorescent reporter molecule to the muscle nicotinic acetylcholine (ACh) receptor (nAChR) at the 272 position of the β subunit (commonly designated $\beta 19'$).¹ We introduced a Cys mutant at this position that we were able to specifically label with a tetramethylrhodamine (TMR) methane thiosulfonate (MTS) compound. Since this site is only accessible in the presence of ACh, we could passivate endogenous cysteines with other MTS reagents and then apply TMR-MTS in the presence of ACh to label the channel at the $\beta 19'$ position. These labeled receptors permitted us to measure conformational events associated with agonist binding to the α/δ binding interface. These events were electrophysiologically silent, occurring in response to the binding of a single ligand, which is insufficient to open the channel. These experiments have been published in Dahan *et al.*¹ Constructs and labeling protocols have subsequently developed for the other subunits in the nAChR pentamer.² Here we describe work done in support of these studies in which photoactivatable nAChR agonists were prepared to enable rapid agonist application.

A schematic representation of the states of the nAChR involved in gating is given in Figure 1. This is a rather simplistic scheme, but one sufficient to represent all of the events observed in our experiments (schemes with over one hundred different receptor states have been proposed).³ The channel begins in a closed, unliganded state (Fig. 1, C). When two agonists bind to the channel, this induces channel gating and ion flow (Fig. 1, State OA_2). This is a metastable state of the receptor however, and these channels rapidly move to the global energetic minimum in the presence of ligand, the desensitized state (Fig. 1, DA_2). This state corresponds to a doubly-liganded channel through which no ions can flow. This state is similar to the singly-liganded, closed state of the receptor (Fig. 1, CA) which we, for the first time, observed in these studies. We wished to make certain that the non-conducting fluorescent state we observed in fact corresponded to the situation shown in CA and not to

direct transit from C to DA₂. The fluorescent properties of the singly-liganded, unopened state CA, the doubly-liganded open state OA₂, and the desensitized state DA₂ are indistinguishable in our experiments. Thus we had to find another way to distinguish CA from DA₂.

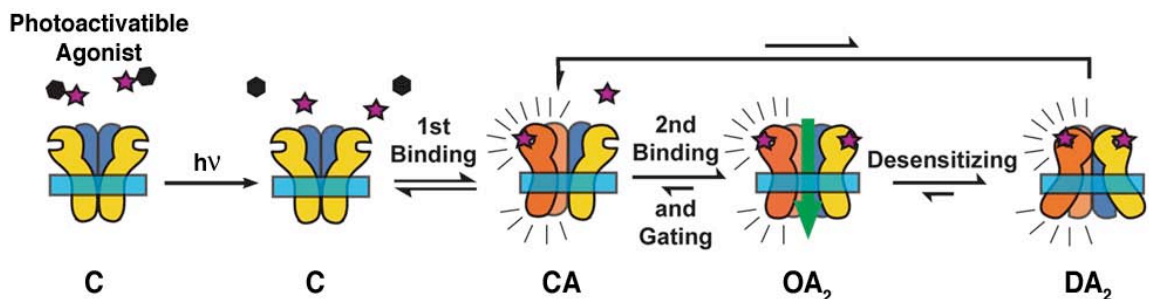
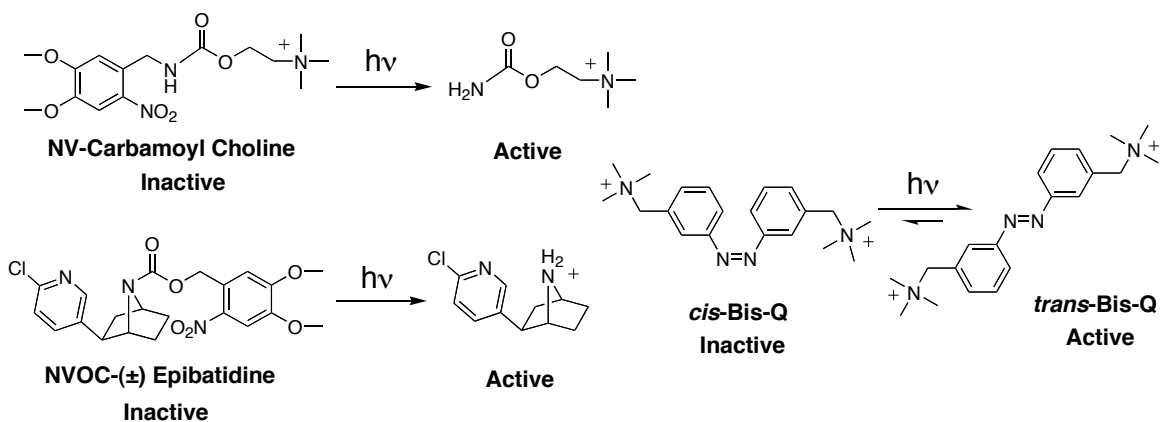


Figure 1. nAChR Gating Mechanism. From left to right: Agonist molecules are in inactive state, channel is closed (C), fluorescence is low; agonist molecules are activated by irradiation; one agonist molecule binds to channel, fluorescence increases, channel is still closed (CA); second agonist molecule binds, channel in high fluorescence state, ions flow through open pore (OA₂); receptor desensitizes (DA₂), still highly fluorescent, but no ions flow.

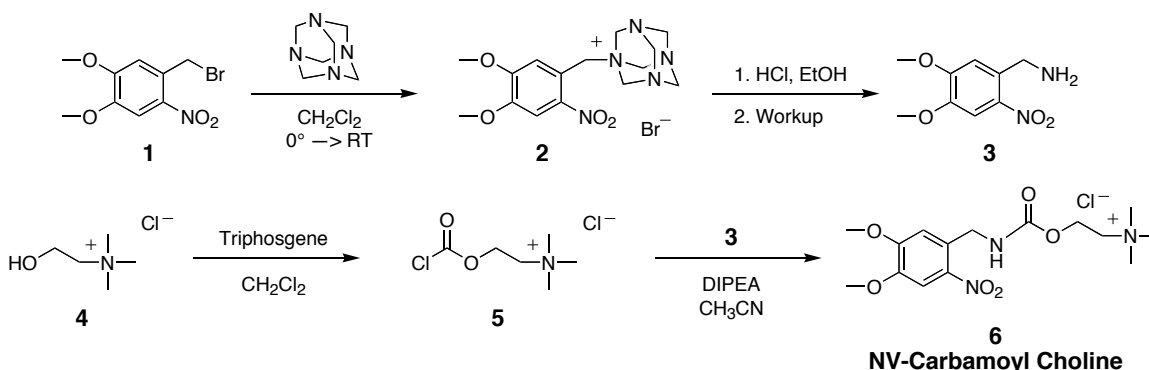
The timecourses of fluorescence changes (ΔF) could be fit by a double exponential. The slow phase of ΔF had the same time constant as the change in current (ΔI) associated with desensitization, on the order of 10 s. To demonstrate that the fast phase of ΔF was not due to rapid desensitization, we needed apply agonist much more rapidly than this. Unfortunately, solution exchange around an oocyte cannot be performed sufficiently rapidly. However, photochemical processes can take place on the ns to ms timescale.⁴ We sought to use photoactivatable agonists, which can be driven from an inactive (with respect to gating the channel) to an active state, to rapidly change the effective agonist concentration in the media.



Scheme 1. Photoactivation of nAChR Agonists.

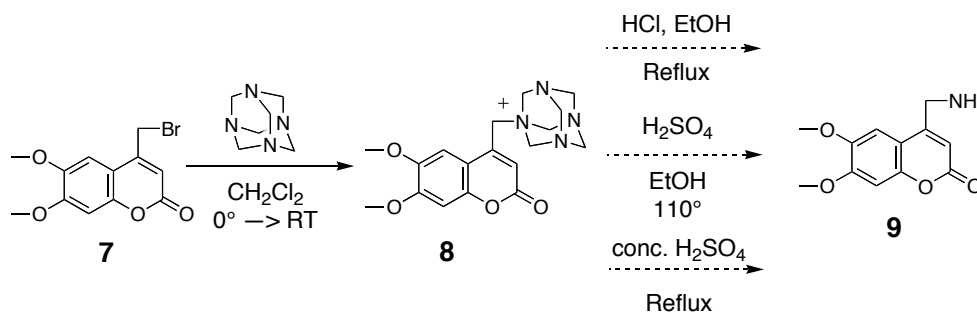
Nitrobenzyl-caged carbamoyl choline, a commercially photoactivatable agonist was employed, and the related nitroveratryl (NV)- and dimethoxycoumarinyl (DMCm)-carbamoyl cholines were synthesized. We synthesized these compounds because the nitrobenzyl protecting group on the commercially available caged carbamoyl choline is photolyzed by 300 nm light, a wavelength that interferes with the fluorescent measurements being made.⁵ The NV and DMCm moieties absorb near 350 nm.⁶ Nitroveratryl oxycarbonyl (NVOC)-(\pm)epibatidine was also synthesized. Although some trial photolyses seemed promising, none of these compounds proved suitable to our purposes. Instead, we employed Bis-Q, a photoisomerizable agonist known to activate the channel much more rapidly than it causes desensitization. Although this has been prepared before^{7, 8}, we describe here current methods for photoisomerizing to its inactive state and storing it thusly.

The synthesis of NV-carbamoyl choline (**6**) was straightforward, following a procedure from Milburn *et al.*⁹ Treatment of nitrobenzyl bromide **1** with hexamethylene tetramine followed by acidolysis gave nitrobenzyl amine **3**. Choline chloroformate (**5**) was synthesized in one step and combined with **3** to give **6**, which was purified by HPLC.



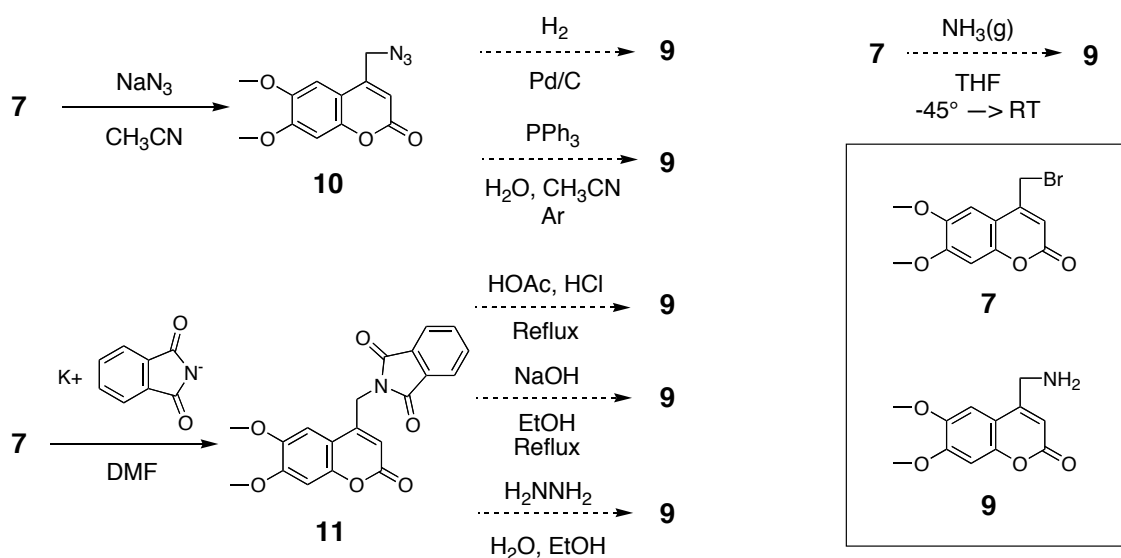
Scheme 2. Synthesis of NV-Carbamoyl Choline.

The synthesis of the analogous dimethoxycoumarin-caged compound proved much more complicated. Although we were able to form the utropine adduct **8**, we were not able to decompose the tetramine moiety to form **9**.



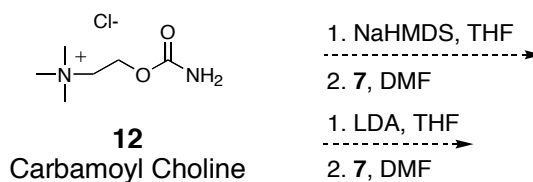
Scheme 3. Attempted Syntheses of DMCm-Carbamoyl Choline.

Similarly, attempts to form **9** through azide reduction, direct amination from ammonia gas, or Gabriel chemistry also failed.



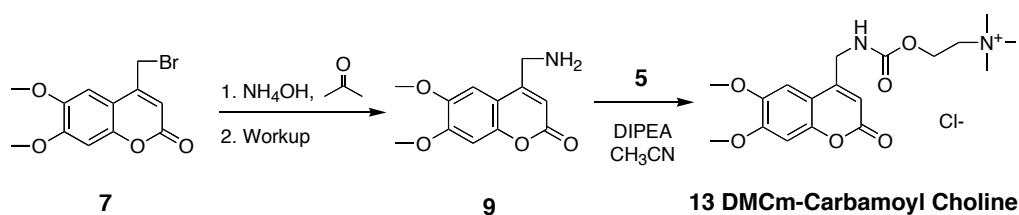
Scheme 4. Attempted Syntheses of DMCm-Carbamoyl Choline.

We also attempted to synthesize DMCm-carbamoyl choline by directly alkylating carbamoyl choline (**12**), but we only observed hydrolysis of the carbamate group.



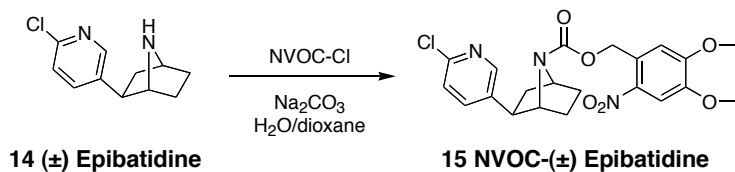
Scheme 5. Attempted Syntheses of DMCm-Carbamoyl Choline.

Although direct amination by bubbling ammonia gas failed, we found that we were able to aminate **7** by treatment with ammonium hydroxide in a procedure adapted from Onderwater *et al.*¹⁰ This could then be elaborated to **13** by reaction with **5**, and then purified by HPLC.



Scheme 6. Synthesis of DMCm-Carbamoyl Choline.

The synthesis of NVOC-epibatidine (**11**) was also quite simple. Standard amide formation procedures were used to protect the secondary amine using nitroveratryl oxycarbonyl chloride (NVOC-Cl).



Scheme 7. Synthesis of NVOC-Epibatidine.

We tested the photolysis of these compounds by examining changes in their HPLC elution times and mass spectra. When NV-carbamoyl choline was run on the HPLC prior to irradiation, two peaks were observed, one at 1.4 min. that only showed absorbance in the UV at 220 nm and one that absorbed at 220, 260, and 350 nm at 12.1 min. (Fig. 2) The peak at 1.4 min. could have come from carbamoyl choline, which had been degraded under ambient light. As the product had been HPLC purified ($t_{\text{elution}} = 12$ min.), we felt secure that it could not have come from a lack of purity in our initial sample. It may simply be an air bubble, as no HPLC peak with a UV trace corresponding to nitroveratraldehyde, the other photolysis product (UV absorption maximum at 380 nm), can be seen. However, we never addressed this issue because we were unable to decage **6** on a timescale suitable to our fluorescence applications. 1 s of irradiation failed to liberate much of our caged compound, as judged by the significant peak that remains at 12.1 min. The peak generated at 10.4 min. does correspond to nitroveratraldehyde in its UV spectrum and retention time (verified by photolysis of other NV-caged compounds). The Hg arc lamp (normally used for decaging protected aminoacyl tRNAs) used in this test was much more powerful than the lamp used for decaging on the electrophysiology rig, and 1 s of irradiation was still an unacceptably long time. After 10 min. of irradiation, **6** could no longer be observed, but substantial decomposition was also observed. Thus NV-carbamoyl choline was deemed unacceptable as a caged agonist.

DMCm-carbamoyl choline also did not appear to degrade readily under the Hg arc lamp. Despite the fact that it was HPLC-purified and that its NMR spectrum looked relatively clean, the initial ($t_{\text{hv}} = 0$) HPLC trace showed more than one peak. Furthermore, irradiation did not produce new peaks. Application of both **6** and **13** to oocytes with irradiation produced no nAChR currents (data not shown).

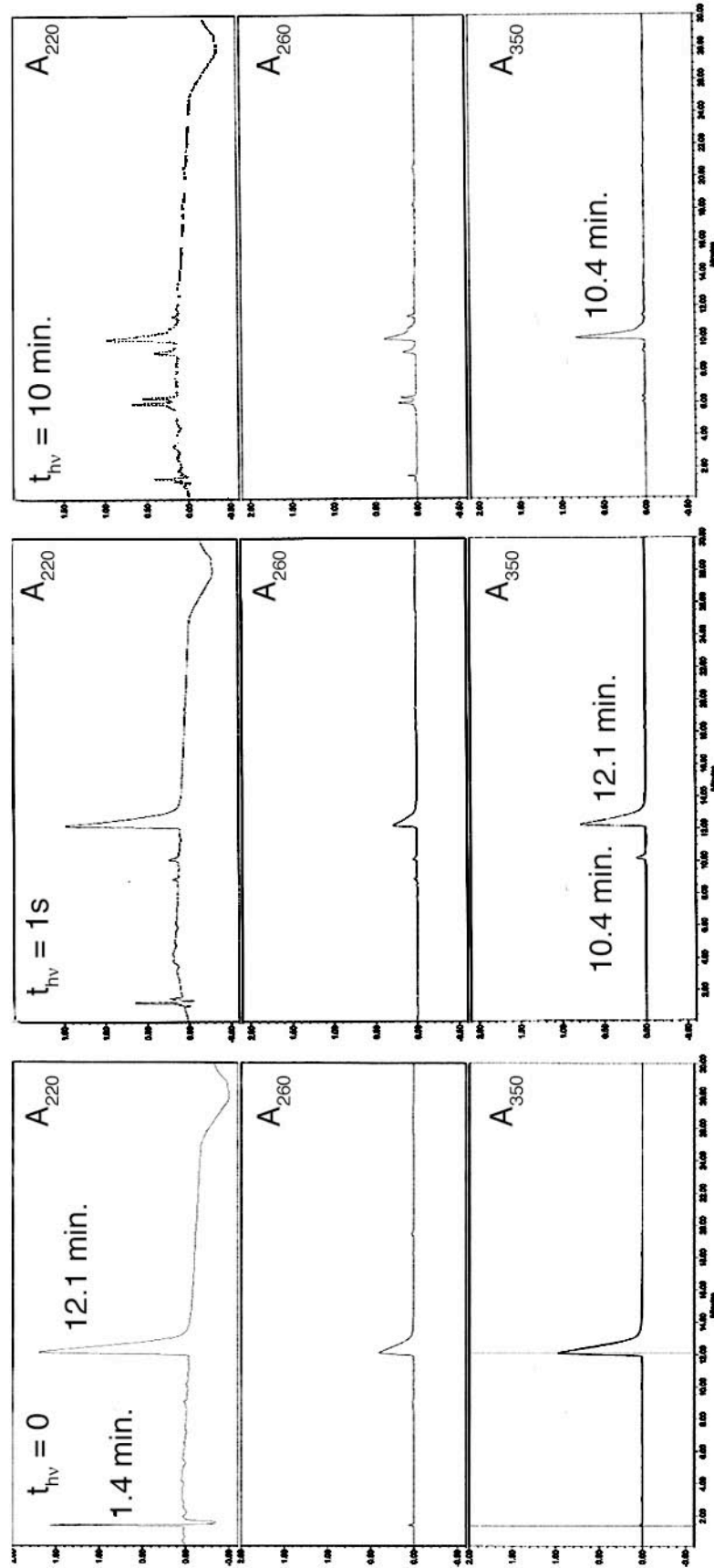


Figure 2. HPLC Monitoring of NV-Carbamoyl Choline. t_{hv} = irradiation time corresponding to given HPLC trace. Other times listed denote HPLC retention times.

NVOC-Epipatidine produced much more favorable results. Irradiation for 1s with the Hg arc lamp cleanly converted the NVOC-epibatidine from caged to decaged form, as judged by HPLC and MS.

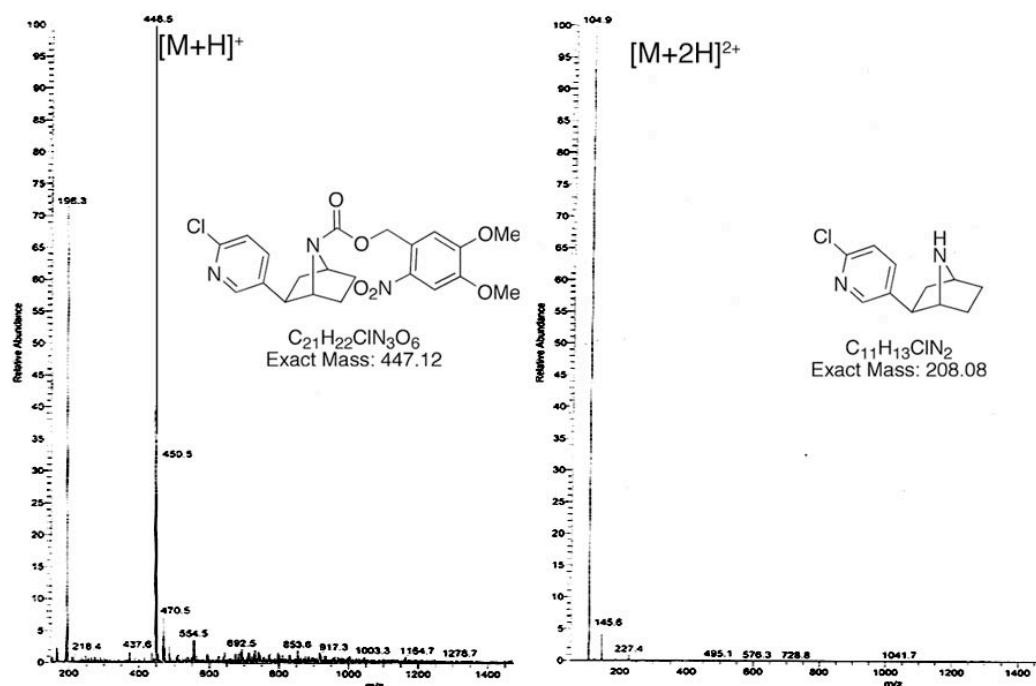


Figure 3. Decaging of NVOC-Epipatidine as Monitored by MS.

However, when used in trial electrophysiology runs, **15** was found to induce currents in its caged form (a very surprising result given our studies of the epibatidine binding modes in Chapters 4 and 5). Furthermore, no additional current was observed upon irradiation. This may be due to receptor desensitization, a well-characterized phenomenon with uncaged epibatidine.¹¹

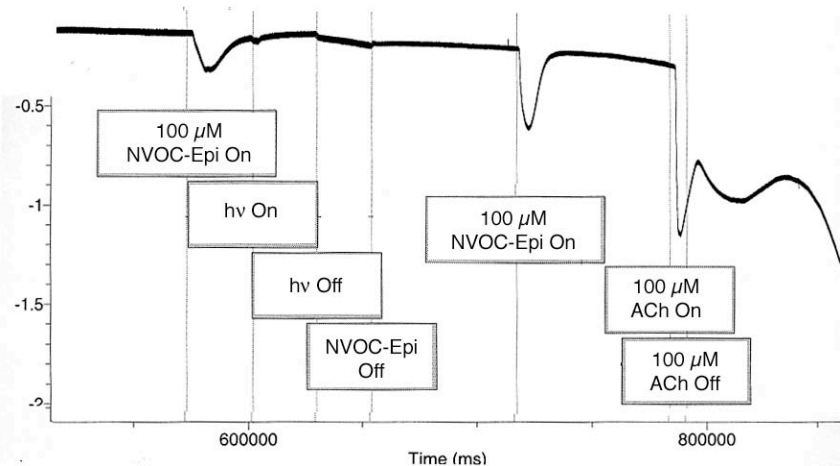
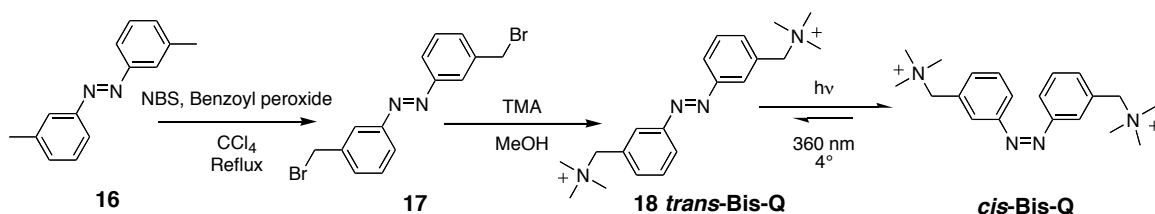


Figure 4. Application of NVOC-Epipatidine to Oocytes Expressing Wild Type nAChRs.

Given the difficulty of photolyzing the caged epibatidine compound on the electrophysiology rig and the desensitization issues surrounding its use, we turned to a photoisomerizable agonist, Bis-Q. Bis-Q was known to convert from its inactive (*cis*) to its active (*trans*) state with at least ms time resolution, and it was known not to cause substantial receptor desensitization.^{7, 8} The only drawback to Bis-Q, which lead us to try these other caged agonists first, is that it is a very weak partial agonist of the nAChR. The synthesis and purification of the inactive *cis*-Bis-Q have been described before, so we will only comment on a few observations that seem inconsistent with the literature precedent.^{7, 8} (See Material and Methods for a description of our updated protocol.)



Scheme 8. Synthesis and Photoisomerization of Bis-Q.

Photoisomerization and chromatographic purification of *cis*-Bis-Q proceeded in keeping with the literature. UV spectra of the photostationary state (following irradiation at 350 nm) and the purified *cis* and *trans* products are shown in Figure 5.

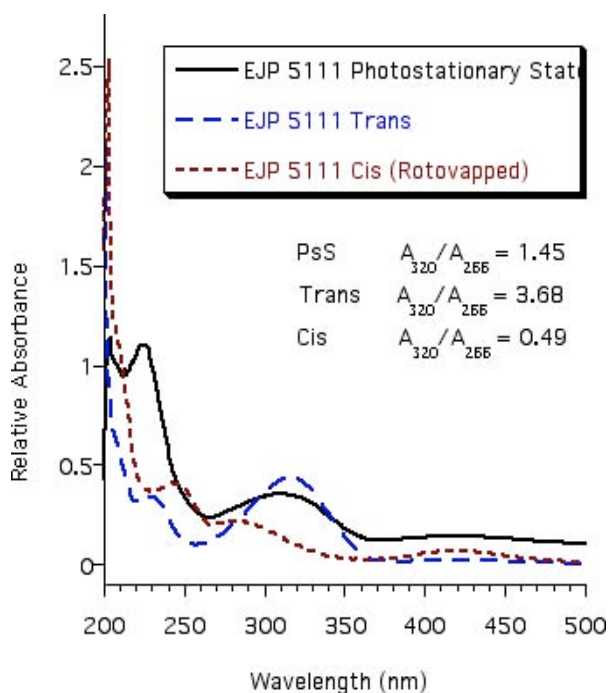


Figure 5. UV Spectra of Various Bis-Q Mixtures. *trans* corresponds to *trans* peak from FPLC purification.

However, we found that once purified, the *cis* compound rapidly equilibrated to a 9:1 *cis/trans* composition, independent of the temperature at which it was stored. Furthermore, the *cis* compound continued to convert back to *trans* when stored in the dark even when frozen. (Fig. 6) In fact, it isomerized more rapidly at -80°C than at room temperature. We found that when the acetonitrile present in the HPLC solvent was removed by rotary evaporation and the compound was stored in dilute solution of ND-96, in the dark, at -20°C , we could maintain 90% purity for about 1 month (data not shown).

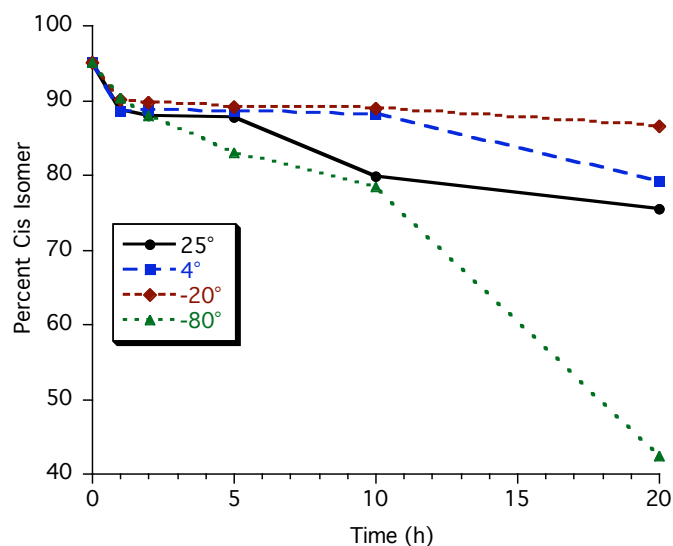


Figure 6. Bis-Q Purification and Storage. Time and temperature dependence of *cis*-Bis-Q purity.

This purified *cis*-Bis-Q was used to determine that the unliganded, nonconducting state we observed prior to channel opening was not the result of fast desensitization and was in fact the electrophysiologically-silent gating movement that we believed it to be. See Dahan *et al.* for a detailed description of this work.¹

Materials and Methods

General

Reagents were purchased from Aldrich, Sigma, or other commercial sources. Anhydrous THF, acetonitrile, and methylene chloride were obtained from J. T. Baker solvent kegs; anhydrous DMF (Puris) was obtained from Fluka. Flash chromatography was on 230-400 mesh silica gel with the solvent indicated. All NMR shifts are reported as δ ppm downfield from TMS. ^1H NMR and ^{13}C NMR spectra were recorded at 300 MHz in CDCl_3 or CD_3CN using a Varian QE-300 spectrometer. Electrospray (ESI) ionization mass spectrometry was performed at the Caltech Protein/Peptide Micro Analytical Laboratory or at the Caltech Division of Chemistry and Chemical Engineering Mass Spectrometry Facility. HPLC purifications were performed on a Waters (Milford, MA) 996 PDA/510 Pump system. FPLC purifications were performed on a Perseptive Biosystems (Framingham, MA) Vision system.

6-Nitroveratryl Amine (**3**)

2.00 g 6-nitroveratryl bromide (**1**) were dissolved in 100 mL CH_2Cl_2 and cooled to 0° in an ice bath. 1.12 g hexamethylene tetramine were dissolved in 50 mL CH_2Cl_2 and cooled to 0° before addition to the solution of **1**. The reaction was stirred for 8 hours at room temperature. The yellow precipitate which formed was filtered (2.54 g, 84% crude yield) and redissolved in 4:1 EtOH/ concentrated HCl. After refluxing overnight (**2** does not dissolve completely until heated), solvent was removed under vacuum. The solid was dissolved in 1M NaOH and extracted 3 times with methylene chloride. Rotary evaporation followed by drying under vacuum gave 0.99 g of **3** (64% yield). ^1H NMR (CD_3CN): δ 7.59 (s, 1H), 7.09 (s, 1H), 4.05 (s, 2H), 3.94 (s, 3H), 3.87 (s, 3H), 1.59 (br s, 2H); ^{13}C NMR (CDCl_3): 153.8, 147.6, 140.2, 134.6, 111.8, 108.3, 56.5, 55.9, 44.7.

Choline Chloroformate Chloride (**5**)

6.63 g choline chloride (**4**) were dried overnight and slurried in 200 mL dry acetonitrile under Ar. 7.05 g triphosgene were dissolved in 50 mL CH_3CN and added to the slurry of **4** via syringe. This was stirred for 10 hours at room temperature. Solvent was removed, and **5** was dried under vacuum. (100% yield by NMR) ^1H NMR (CD_3CN): δ 4.77 (t, $J = 4.7$ Hz, 2H), 3.87 (t, $J = 4.7$ Hz, 2H), 3.24 (s, 9H); ^{13}C NMR (CDCl_3): 149.5, 65.1, 63.6, 53.6.

Nitroveratryl-Carbamoyl Choline Acetate (**6**)

0.495 g **3** were dissolved in 50 mL dry acetonitrile under Ar and cooled to 0° C. 0.943 g **5** were slurried in 200 mL CH_3CN under Ar. 0.2 mL dry *N,N,N*-diisopropylethylamine was added to the solution of **3** via syringe. The slurry of **5** was added slowly with a wide bore cannula. The reaction was warmed to room temperature and

stirred for 3 hours. After rotovapping to dryness, the mixture was dissolved in 10 mL of water and purified by reverse phase HPLC with the following gradient:

t (min.)	% 25 mM NH ₄ OAc aq.	% CH ₃ CN
0	95	5
22	60	40
25	5	95

One major peak was observed, with a large UV absorbance at 220 nm and 350 nm. This peak was collected and solvent was removed by lyophilization. This was redissolved and lyophilized from 10 mM acetic acid in water to ensure that all NH₄OAc was removed. Thus, the compound was obtained as the acetate salt (0.481 g, 51%) NMR peaks from both amide rotamers were identical except for the resonance at ~ 4.6 ppm. ¹H NMR (CD₃CN): δ 7.63 (s, 1H), 7.34 (br s, 1H), 7.10 (s, 1H), 4.62 (Rotamer A) and 4.58 (Rotamer B) (s, 2H), 4.43 (t, J = 3.3 Hz, 2H), 3.92 (s, 3H), 3.87 (s, 3H), 3.61 (t, J = 3.3 Hz, 2H), 3.15 (s, 9H), 1.88 (OAc-) (s, 3H); ¹³C NMR (CDCl₃): 175.3, 155.9, 153.8, 148.0, 140.4, 129.6, 111.8, 108.4, 65.4, 58.5, 56.4, 54.1, 42.5, 22.4. ESI-MS: [M]⁺ 342.2 (obsd), 342.2 (calcd).

Dimethoxycoumarin Methylamine (9)

100 mg dimethoxycoumarin bromide (7) were dissolved in 50 mL acetone and 2 mL concentrated NH₄OH. This was stirred for 3 hours at room temperature. Although the reaction was incomplete as assayed by TLC, the solution was acidified to pH 6 with 6 N HCl and acetone was removed. The remaining aqueous solution was washed twice with CH₂Cl₂ and then basified with Na₂CO₃ to pH 10. This was then extracted three times with EtOAc. The EtOAc layers were combined and diluted 1:1 with isopropanol. 10 drops of concentrated HCl and 5 mL of pentane were added, and the solution was set aside overnight to crystallize. The brown precipitate that resulted was collected by filtration and taken on despite its impurity (See NMR spectrum, Fig. 6). ESI-MS: [M]⁺ 236.1 (obsd), 236.1 (calcd).

Dimethoxycoumarin-Carbamoyl Choline Acetate (13)

50 mg **9** were dissolved in 60 mL dry acetonitrile under Ar and cooled to 0° C. 100 mg **5** were slurried in 20 mL CH₃CN under Ar. 0.15 mL dry *N,N,N*-diisopropylethylamine was added to the solution of **3** via syringe. The slurry of **5** was added slowly with a wide bore cannula. The reaction was stirred at 0° for 30 minutes, warmed to room temperature, and stirred for overnight. After rotovapping to dryness, the mixture was dissolved in 8 mL of DMF and purified by reverse phase HPLC with the gradient used for purification of **6**, above. The product (**13**), one of a series of peaks, eluted at 6.8 minutes. As before, it was lyophilized to a solid and then re-lyophilized from a 10mM acetic acid solution. ESI-MS: [M]⁺ 365.2 (obsd), 365.2 (calcd) (Another, unexplained peak was observed at 502.2)

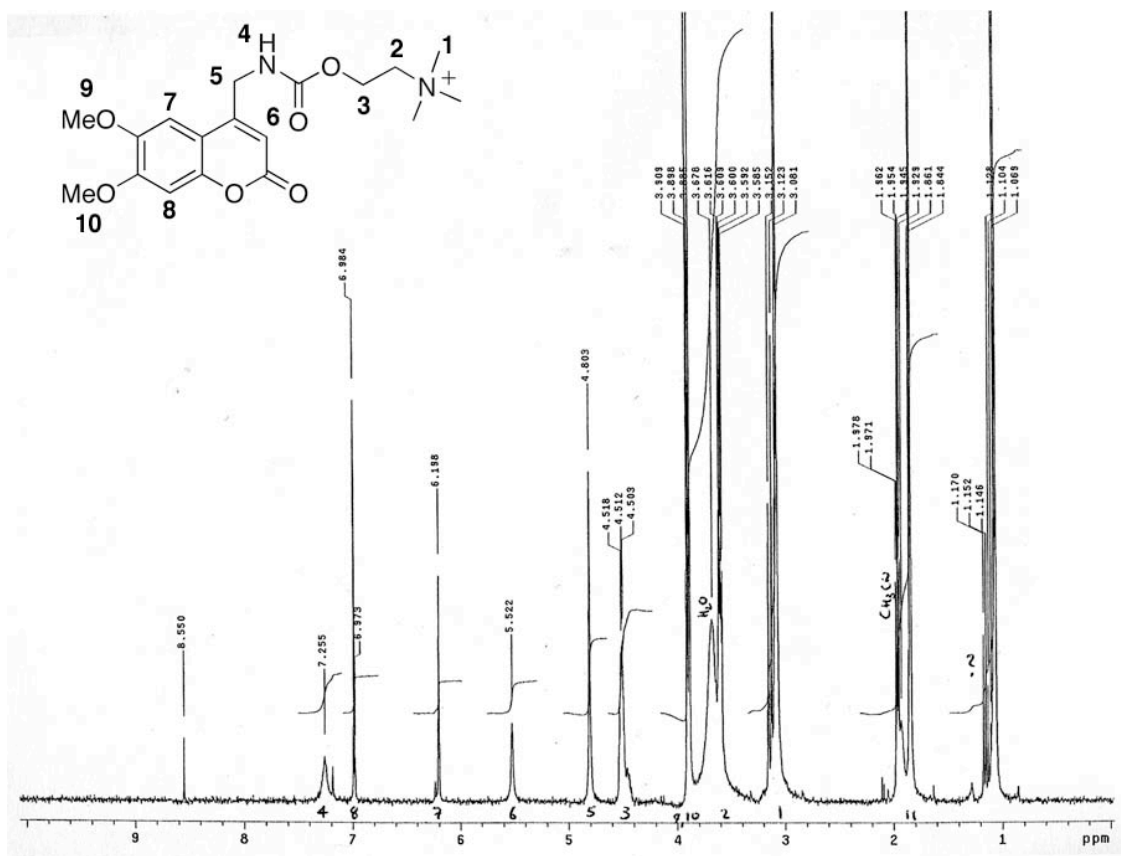
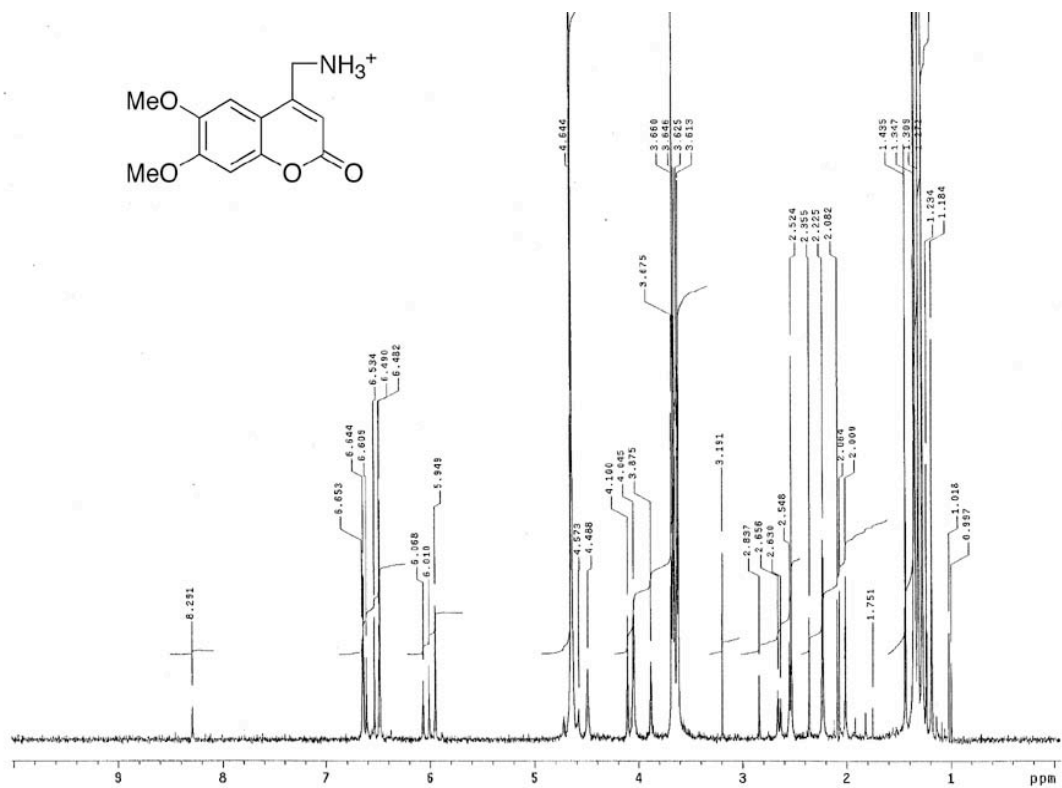


Figure 7. 300 MHz NMR Spectra of **9** in D_2O (Top) and **13** in CD_3CN (Bottom).

NVOC-Epibatidine (**15**)

10 mg (\pm)epibatidine (**14**) were dissolved in 5 mL *p*-dioxane and 5 mL water. 3 mL of a solution of 38 mg Na₂CO₃ in 10 mL water (the 3 mL represents 3 equivalents) were added to the solution of **14**. 27 mg 6-nitroveratryl oxycarbonyl chloride (NVOC-Cl) were dissolved in 5 mL dioxane, and were added to the other mixture and stirred for 2 hours. TLC analysis showed that the reaction was complete. The reaction mixture was basified with 1M Na₂CO₃ and extracted with 3 X 25 mL CH₂Cl₂, the organic layers were combined, dried with sodium sulfate, and run on a column in 2:1 petroleum ether/EtOAc to give 15 mg (100% yield) of product. ¹H NMR (CDCl₃): δ 8.26 (s, 1H), 7.69 (s, 1H), 7.59 (d, J = 8.8 Hz, 1H), 7.26 (d, J = 8.8 Hz, 1H), 6.92 (s, 1H), 5.48 (s, 2H), 4.51 (m, 1H), 4.27 (m, 1H), 3.97 (s, 3H), 3.94 (s, 3H), 3.34 (m, 1H), 2.04 (AB, J = 8.7 Hz, J = 11.4 Hz, 2H), 1.70 (m, 2H), 1.63 (m, 2H); ¹³C NMR (CDCl₃): 154.0, 153.4, 149.7, 148.7, 139.8, 137.3, 132.5, 127.5, 124.4, 110.8, 108.5, 64.5, 63.1, 62.7, 56.8, 56.6, 45.3, 40.3, 30.1, 29.2. ESI-MS: [M+H]⁺ 448.5 (obsd), 448.5 (calcd).

Photolysis Trials

Photolyses of **6**, **13**, and **15** were conducted on \sim 1 μ M solutions in 10:1 distilled water / acetonitrile. Irradiation was performed with a 1000 W Hg/Xe arc lamp (Oriol, Stratford, CT) operating at 400 W equipped with WG-335 and UG-11 filters (Schott, Elmsford, NY). The outcome was monitored by HPLC and ESI-MS (1% AcOH acid added for ESI⁺). Electrophysiological monitoring of the decaging of **15** was performed on the apparatus described in the supplemental information accompanying Chapter 7.

Bis-Q Purification

trans-Bis-Q :¹H NMR (DMF-d₆ and D₂O): δ 8.32 (s, 2H), 8.10 (d, J = 8.0 Hz, 2H), 7.99 (d, J = 8.0 Hz, 2H), 7.99 (d, J = 8.0 Hz, 2H), 7.83 (dd, J = 8.0 Hz, J = 8.0 Hz, 2H), 5.09 (s, 4H), 3.43 (s, 18H); ¹³C NMR (DMF-d₆ and D₂O): 152.7, 136.5, 130.5, 128.4, 128.2, 123.9, 67.8, 52.5. ESI-MS: [M]²⁺ 163.1 (obsd), 163.1 (calcd); [M-2NMe₃+H]⁺ 209.1 (obsd), 209.1 (calcd); [M-NMe₃]⁺ 268.1 (obsd), 268.1 (calcd); [M-Me]⁺ 311.2 (obsd), 311.2 (calcd); [M+I-NMe₃]⁺ 394.0 (obsd), 394.0 (calcd); [M+I]⁺ 452.9 (obsd), 452.9 (calcd).

Adapted from Nerbonne *et al.*⁸: 29 mg Bis-Q iodide were dissolved in 5.0 mL distilled water and irradiated overnight at 4° C with a Blak-Ray B-100 lamp (UV Products, Inc., San Gabriel, CA). This was run on the FPLC with a Partisil (Whatman, Clifton, NJ) 5P1139 ODS-3 column using the following buffers and gradient:

Buffer A: 0.1 M NaCl, 0.1% HCl, pH adjusted to 4.0 with NaOH.

Buffer B: 60% acetonitrile in 0.1 M NaCl, 0.1% HCl.

t (min.)	% Buffer A	% Buffer B
0	100	0
60	50	50
70	0	100

Two peaks were observed, which can be seen in the following trace:

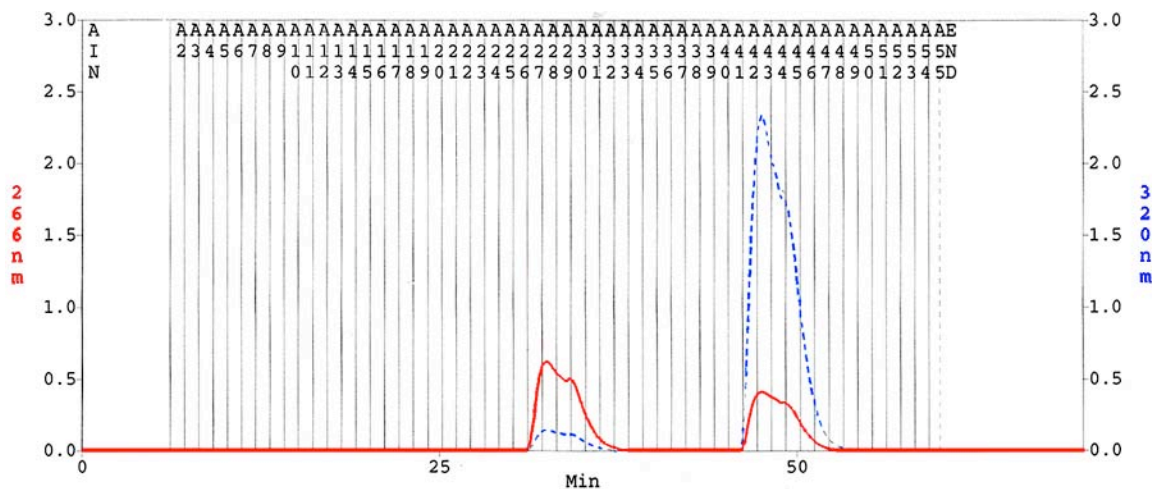


Figure 8. FPLC Trace of a Bis-Q Purification Run. Divisions indicate fractions collected.

The *cis* peak is first, in a roughly 3:2 ratio based on the UV absorption at 266 nm, the isobestic point. *cis/trans* ratios for the product were computed with UV and the following equation:

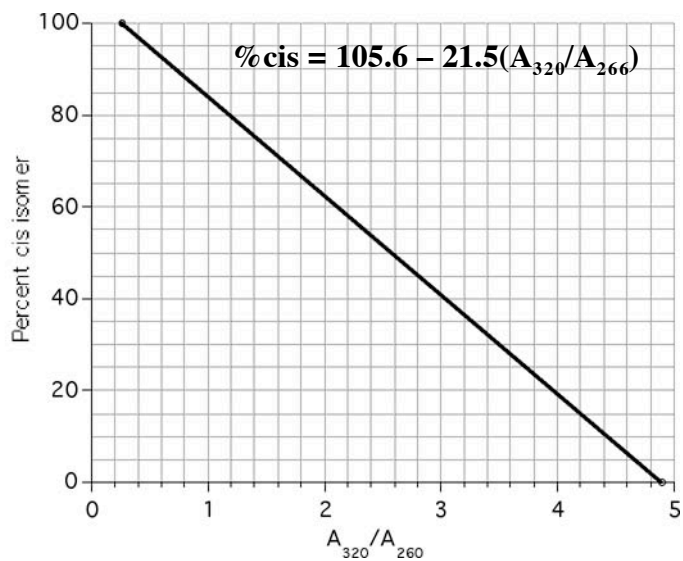


Figure 9. Bis-Q *cis/trans* ratio vs. A_{320}/A_{266}

Acetonitrile was removed by rotovapping at room temperature in the dark, and the compound was stored at roughly 300 μ M in ND-96 the dark at -20 °C.

References

- (1) Dahan, D. S.; Dibas, M. I.; Petersson, E. J.; Auyeung, V. C.; Chanda, B.; Bezanilla, F.; Dougherty, D. A.; Lester, H. A., *Proc. Natl. Acad. Sci. USA* **2004**, 101, 10195-10200.
- (2) Dibas, M. I. Unpublished Results
- (3) Changeux, J. P.; Edelstein, S. J., *Neuron* **1998**, 21, 959-980.
- (4) Hess, G. P.; Grewer, C., *Methods Enzymol.* **1998**, 291, 443-473 Niu, L.; Vazquez, R. W.; Nagel, G.; Friedrich, T.; Bamberg, E.; Oswald, R. E.; Hess, G. P., *Proc. Natl. Acad. Sci. USA* **1996**, 93, 12964-12968.
- (5) Gee, K. R.; Carpenter, B. K.; Hess, G. P., *Methods Enzymol.* **1998**, 291, 30-50.
- (6) Furuta, T.; Iwamura, M., *Methods Enzymol.* **1998**, 291, 50-63.
- (7) Lester, H. A.; Nass, M. M.; Krouse, M. E.; Nerbonne, J. M.; Wassermann, N. H.; Erlanger, B. F., *Ann. N.Y. Acad. Sci.* **1980**, 346, 475-490.
- (8) Nerbonne, J. M.; Sheridan, R. E.; Chabala, L. D.; Lester, H. A., *Mol. Pharmacol.* **1983**, 23, 344-349.
- (9) Milburn, T.; Matsubara, N.; Billington, A. P.; Udgaonkar, J. B.; Walker, J. W.; Carpenter, B. K.; Webb, W. W.; Marque, J.; Denk, W.; Mccray, J. A.; Hess, G. P., *Biochem.* **1989**, 28, 49-55.
- (10) Amer Chemical Soc Onderwater, R. C. A.; Venhorst, J.; Commandeur, J. N. M.; Vermeulen, N. P. E., *Chem. Res. Toxicol.* **1999**, 12, 555-559.
- (11) Badio, B.; Daly, J. W., *Mol. Pharmacol.* **1994**, 45, 563-569 Dukat, M.; Glennon, R. A., *Cell Mol. Neurobiol.* **2003**, 23, 365-378.

Section 3: Chapter 11

Application of Tethered Agonist Methods to the 5-HT₃ Receptor

The success we experienced in using the tyrosine-based tethered agonist unnatural amino acids in characterizing the binding site of the nAChR (Chapter 2) lead us to attempt to apply the technique to a related receptor, the 5-HT₃ receptor (5HT₃R). The 5HT₃R is also a member of the Cys-loop family of receptors, one which gates in response to serotonin (5-HT).¹ At the time that our studies began, two types of 5HT₃R subunit had been identified: A and B. The 5HT_{3A}R can form functional homopentamers. The 5HT_{3B}R is not functional on its own, but can form functional heteropentamers with the A subunit. Many of the features of the muscle nAChR binding domain are conserved in the 5HT_{3A}R; including α Trp 149, which we identified as forming a cation- π interaction essential to ligand-binding in the nAChR. Trp 149 aligns with Trp 183 of the 5HT_{3A}R (Fig. 1).

```

5HT3A_Mouse  DEKNQVLTTYIWYRQ YWTDEFLQWTPED-- FDNVTKLSIPTDSIW VPD-ILIN--EFVDV
nAChA_Mouse  DEVNQIVTTNVRLRQ QWVDYNLKWNPDD-- YGGVKKIHIPSEKIW RPDVVLW--NADGD
nAChG_Mouse  NEREEALTTNVWIEM QWCDYRLRWDPKD-- YEGLWILRVPSTMVW RPDIVLEN--NVDGV
AchBP_Snail  NEITNEVDVVFWQQT TWSDRTLAWNSS--- HSPDQVSVWP-ISSW VPDLAWIN---AISK
               $\gamma$ 55/857                                 $\alpha$ 93

5HT3A_Mouse  LDIYNFPFDVQNCSL TFTSWLHTIQDINIT LWRSPEE-----V RSDKSIFINQGEW--
nAChA_Mouse  IIVTHFPFDEQNCSM KLGTWTYDGSVVAIN PESDQ----- -PDLSNFMESGEWVI
nAChG_Mouse  ISVTYFPFDWQNCSL IFQSQTYSTSEINLQ LSQEDGQ---AIEWI FIDPEAFTENGEWAI
AchBP_Snail  VSGVDTESG-ATCRI KIGSWTHSREISVD PTTEN-----S -DDSEYFSQYSRFEI
               $\alpha$ 149

```

Figure 1. Sequence Alignment of 5HT_{3A}R, Muscle nAChR and AChBP. Conserved binding site residues are highlighted and key residues of the aromatic box are denoted with their nAChR numbering.

In work described in Beene *et al.*, a cation- π interaction between 5HT_{3A}R Trp 183 and the primary ammonium of 5-HT was identified.² As in the nAChR studies described in Chapter 2, the F-Trp series was incorporated and dose-response relations were measured. We generate a fluorination plot by plotting the logarithm of the ratio of the mutant EC₅₀ to the wild type EC₅₀ against the calculated binding energy of a probe Na⁺ cation to indoles with various degrees of fluorination (Fig. 2, See Chapter 2 for more details). We can see from the fluorination plot that there is a straight line relationship between the calculated binding energy and the change in the EC₅₀ with fluorination. This is consistent with a cation- π interaction for 5-HT. Moreover, this line has a steeper slope than the ACh fluorination curve, which is consistent with the stronger cation- π interaction expected for a primary ammonium relative to the quaternary ammonium of ACh.

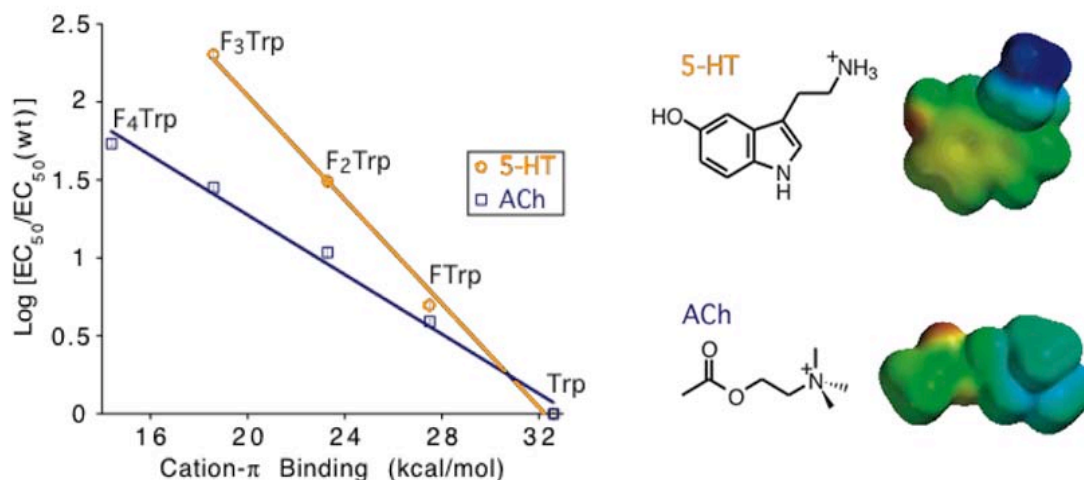


Figure 2. Identification of a Cation- π Interaction Between 5-HT and 5HT_{3A}R. Left: Fluorination plot for ACh at α Trp 149 of the muscle nAChR and 5-HT at Trp 183 of the 5HT_{3A}R. Right: 5-HT and ACh structures and their electrostatic potential surfaces. Surfaces shown on a colorimetric scale from + 10 to + 130 kcal/mol. Surfaces determined from HF/6-31G** MO coefficients with a 0.002 e/Å³ cutoff.

The binding of the 5-HT ammonium to Trp 183 was consistent with some of the geometries generated in docking studies by the Lummis group.³ Using the original AChBP structure as a template, they made homology models of the binding domain of the 5-HT_{3A}R and docked molecules of 5-HT, generating binding geometries like that shown in Figure 3.

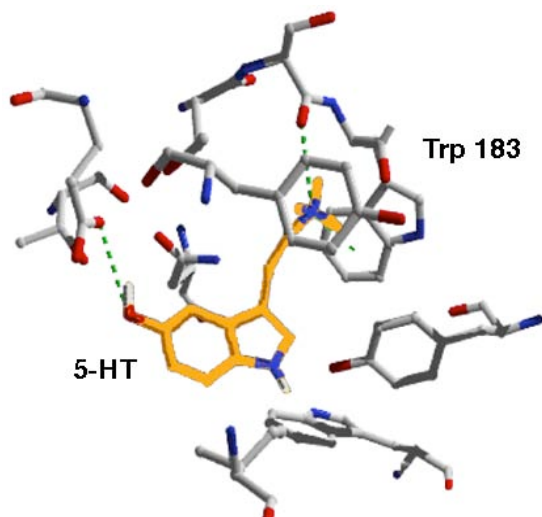


Figure 3. Computational Model of 5-HT Binding to the 5HT_{3A}R. Homology model and docking study performed by Lumis and coworkers. (Reeves *et al.*, 2003)

Since we were able to localize ammonium binding to an aromatic residue in the 5-HT_{3A}R as we were in the nAChR, we sought to employ tethered agonist methodology with this receptor as well. We began using a construct with a TAG mutation at the 183 position and a Ser mutation at a position in the pore-lining TM2 region commonly designated 13' (this is analogous to the 9'S mutation employed in the nAChR studies).⁴ Incorporation of

TyrO3P and TyrO3Q both gave functional receptors. Both tethered agonists yielded receptors with blockable standing currents, showing them to be constitutively active. TyrO3P's standing currents increase at lower media pH, seemingly indicative of the tether modulation observed in the nAChR work. (Fig. 4, Top) However, 5HT_{3A}Rs bearing TyrO3Q show the same pattern of modulation. (Fig. 4, Bottom) This highly specific control demonstrates that the pH modulation does not come from protonation of the primary tether.

Not only does the constitutive behavior appear to be the same amongst the tethered agonist receptors, constitutive activity is also observed in the wild type receptor, with Trp at position 183. (Fig. 5, Top) The constitutive activity of Trp-containing receptors can also be modulated by pH. Notably, although lowering the pH increases constitutive activity, raising the pH to 8.5 does not change constitutive activity.

Like the nAChR tethered agonist receptors, both the TyrO3P and TyrO3Q 5HT_{3A}Rs (13'S) respond to agonist application. The nAChRs responded with some activation, followed by desensitization past the point of zero agonist-induced current. In the 5HT_{3R} study, little desensitization is observed from the tethered agonist receptors. In fact, it is much less severe than the rapid desensitization typically observed with the wild type receptor. As one can see from the top of Figure 5, when 5-HT is applied to the wild type 5HT_{3A}R it causes very rapid desensitization, creating a sharp peak in the current trace.

The source of the constitutive activity in all these receptors seems to be the 13'S mutation itself. Even when tRNA with no amino acid is injected into the oocytes with the mRNA, constitutively active channels are observed. (Fig. 5, Bottom) These channels give virtually no response to 5-HT, but application of QX-314 blocks a substantial amount of current. Apparently, there is sufficient background amino acid incorporation to produce receptors which cannot gate, but can pass Na⁺ ions because of the 13'S mutation. This current too shows some pH modulation.

Two ways of addressing the issue of inherent constitutive activity in the 13'S mutants were addressed. The first used another site that showed the promise of reduced constitutive activity, based on previous work, the 9'V site. Thr mutants at this position were slower to desensitize than wild type receptors. We generated 5HT_{3A}R constructs with TAG mutations at Trp 183 and V9'T mutations. Unfortunately, despite sequencing analysis confirmative of the mutation and agarose gel analysis that showed the mutant mRNA was the right size, no currents were observed from the 9'T mutants. This is not entirely surprising in that vastly reduced channel expression was observed when nAChR receptors with five subunits bearing 9'S mutations are expressed.⁵

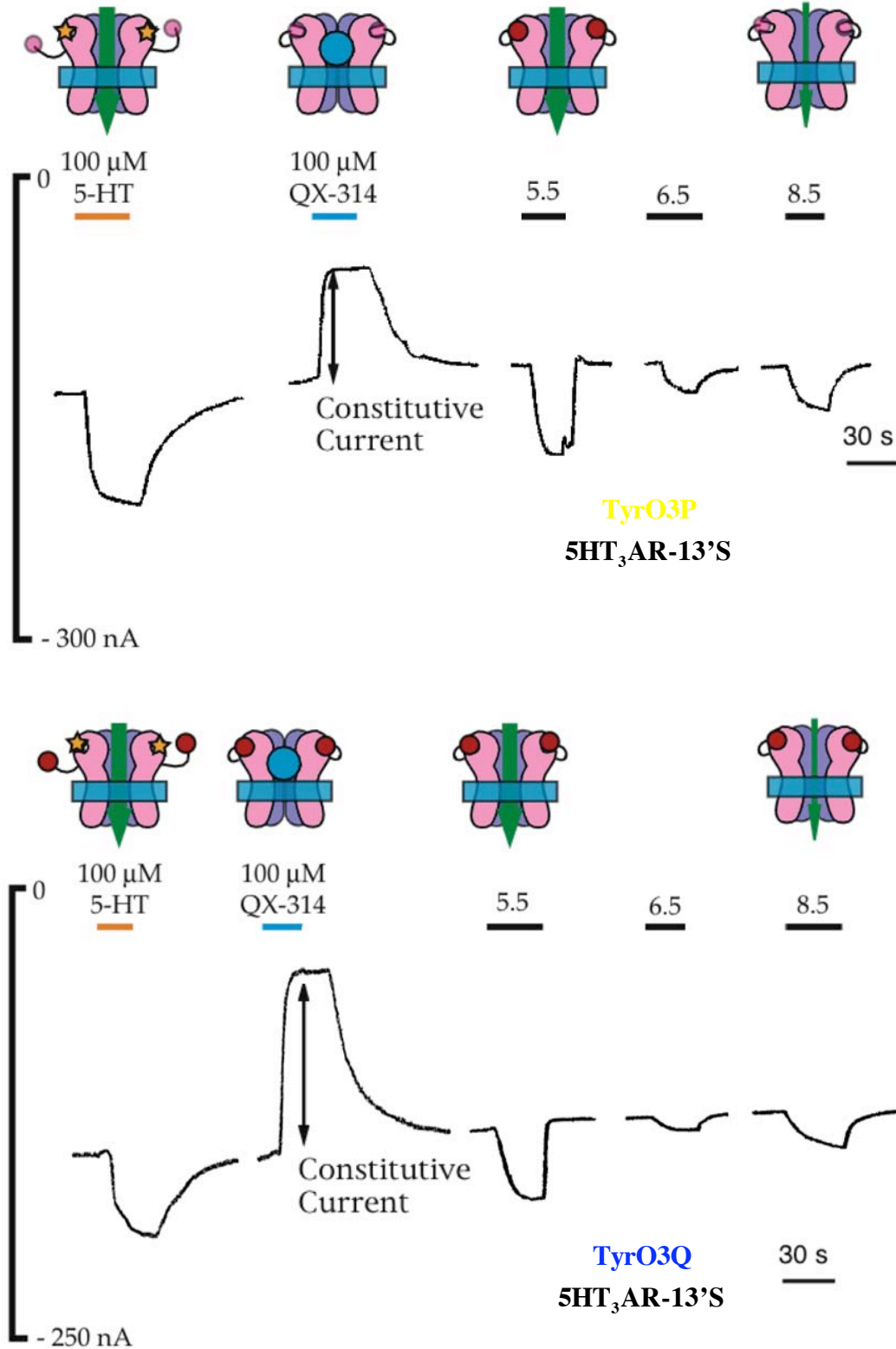


Figure 4. Examples of Electrophysiological Data: TyrO3P and TyrO3Q at 5HT_{3A}R 183. Tethered agonist responses to 5-HT, QX-314, and agonist-free solutions of varying pH. Upper bars indicate application of agonist, blocker, or an agonist-free solutions. Arrows indicate blockable constitutive currents.

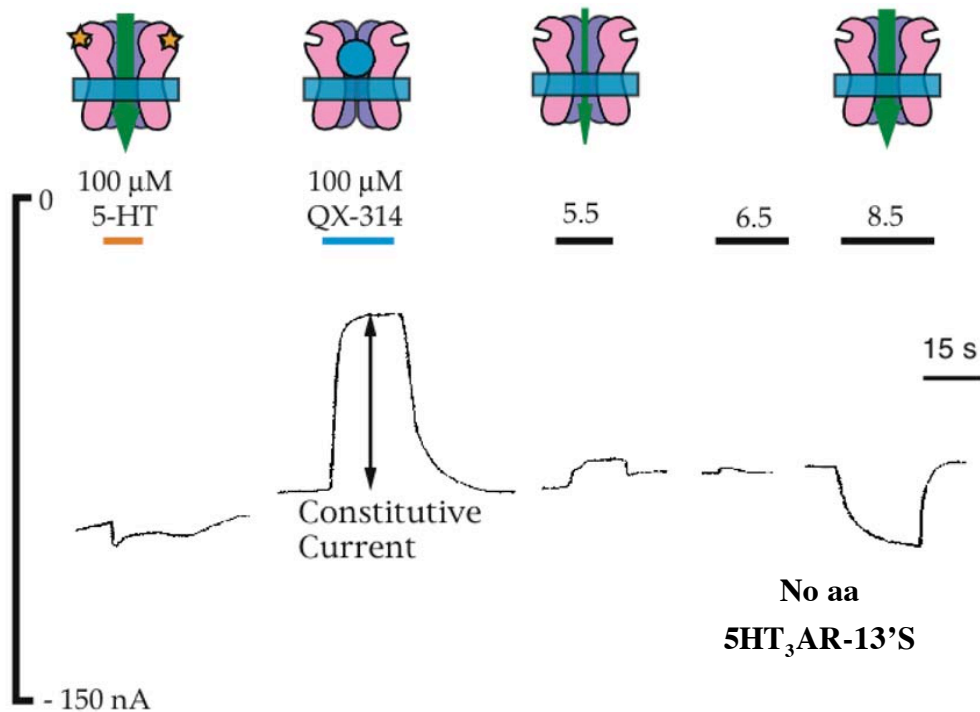
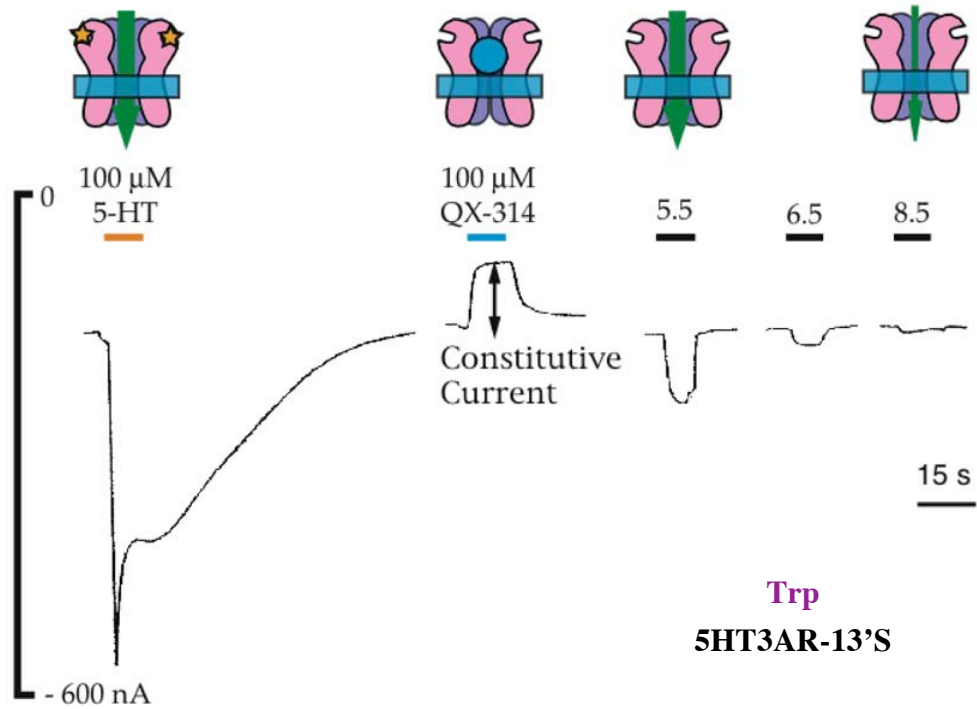


Figure 5. Examples of Electrophysiological Data: Trp and No Amino Acid at 5HT_{3A}R 183. Responses to 5-HT, QX-314, and agonist-free solutions of varying pH. Upper bars indicate application of agonist, blocker, or an agonist-free solutions. Arrows indicate blockable constitutive currents. No amino acid indicates injection of tRNA with no amino acid with 5HT_{3A}R-13'S mRNA.

The second method involved heteropentamers. We sought to reduce the inherent constitutive activity by coexpressing the 13'S 5HT_{3A}Rs with wild type 5HT_{3B}Rs. Studies with the nAChR have shown that the effects of 9'S mutations are additive (in an energetic sense).⁵ In the nAChR, each 9'S mutation decreases the EC₅₀ by an order of magnitude. Each 9' mutation also reduces the Hill coefficient by roughly 0.35, an effect which has been attributed to an increase in mono- and unliganded openings (i.e. constitutive activity).⁵ Thus, it is not surprising that our five-fold 13'S substituted 5HT_{3A}Rs are constitutively active (indeed, there is literature precedent) and we expect to be able to reduce this in a step-wise manner with each wild type 5HT_{3B} subunit that coassembles in the pentamer.⁴ We injected mixtures of 5HT_{3A}Rs (183 TAG, 13'S) and 5HT_{3B}Rs in 2, 5, and 10 to 1 ratios with Trp and TyrO3Q. No active channels were observed in the TyrO3Q experiments. In the studies with Trp at A/B 10:1, some constitutive activity was observed, but it was vastly reduced relative to the 5-HT currents. This is still not a perfect situation, though it seems a sufficiently low background to attempt to observe constitutive activity from a tethered agonist.

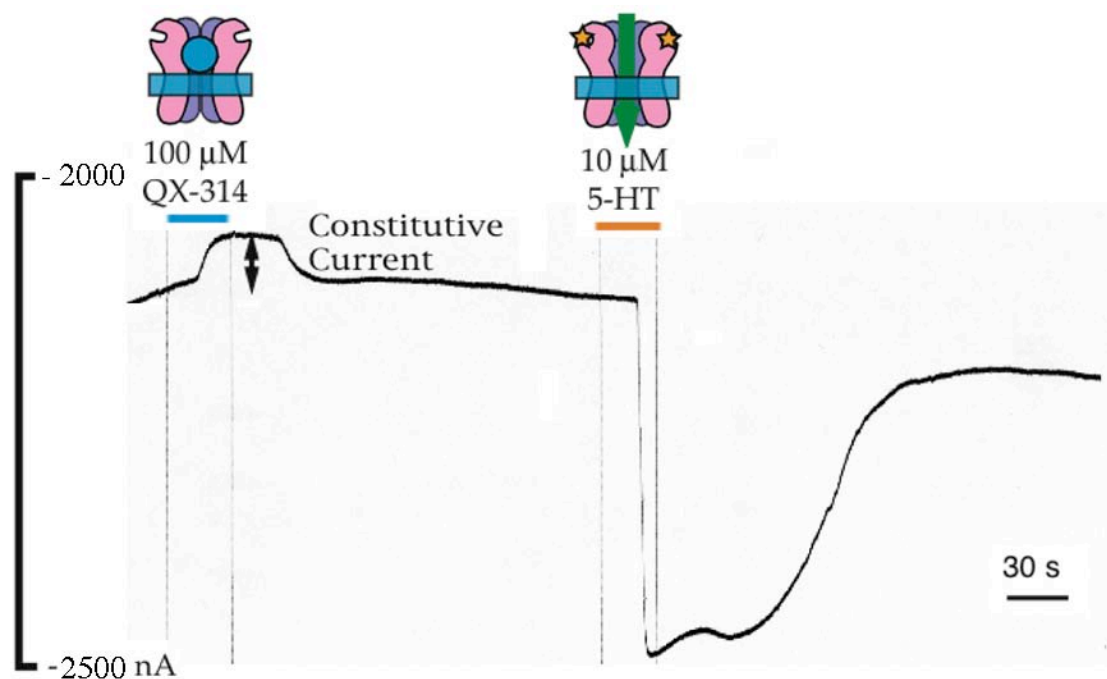


Figure 6. Examples of Electrophysiological Data: Trp Suppression with 10:1 5HT_{3A}R 183 TAG 13'S/5HT_{3B}R. Responses to 5-HT and QX-314. Upper bars indicate application of agonist or blocker. Arrows indicate blockable constitutive currents.

All of the tethered agonists employed in the original nAChR study published in Li *et al.*, TyrOnQ, $n = 2-5$, were tried at 183 with the 10:1 5HT_{3A}(183TAG, 13'S)/_BR mRNA.⁶ Some weak constitutive activity was observed with the four and five carbon tethers, but the

most promising result came from the two carbon tether. These gave large constitutive currents (~ 300 nA) and relatively small 5-HT-induced currents (~ 25 nA). Receptors containing the other tethers did not respond significantly to 5-HT. Importantly, the TyrO2Q-containing 5HT₃R_s responded to 5-HT applications with a brief increase in inward current followed by a slow reduction in inward current that we attribute to desensitization of the receptors. TyrO2Q would have an efficacy of 12 by the criteria employed in the Li *et al.* study, higher than the maximal efficacy observed there, 8 for TyrO3Q at position 149 of the nAChR α subunit.⁶ This seemed to indicate that the two carbon tether is optimal for activating the 5HT₃R at the 183 position, so tethered agonists like TyrO2P should be synthesized to perform a study like the one described in Chapter 3. However, some minimal constitutive activity was still observed from Trp suppression with the 10:1 mixture of A13'S and B subunits.

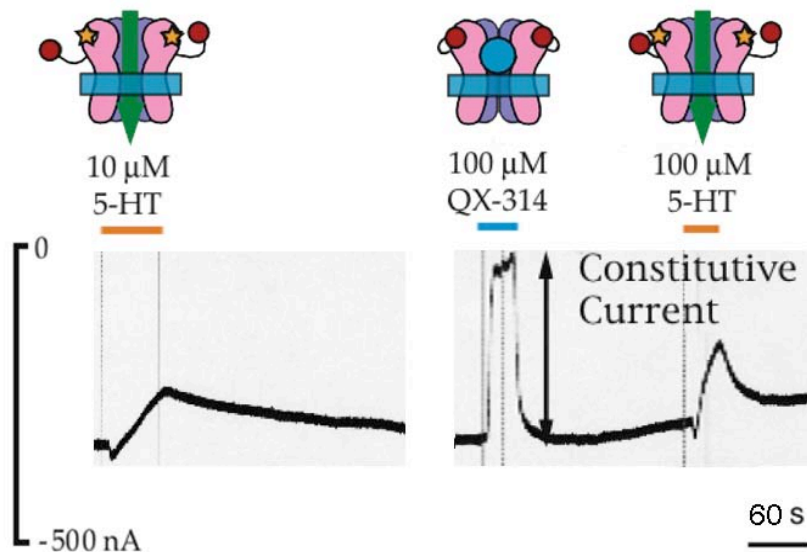


Figure 7. Examples of Electrophysiological Data: TyrO2Q Suppression with 10:1 5HT_{3A}R 183 TAG 13'S/5HT_{3B}R. Responses to 5-HT and QX-314. Upper bars indicate application of agonist or blocker. Arrows indicate blockable constitutive currents.

One further study was performed to seek a system for exploring tethered agonism without background constitutive activity, perhaps one that should have been performed at the beginning of this work: suppression at 183 in an otherwise wild type 5HT_{3A}R. Unfortunately, we observe only very minimal blockable currents with TyrO2Q in this case. Although we see robust currents from Trp suppression, as in the nAChR, tethered agonism does not seem possible in the absence of a TM2 Ser or Thr mutation.

All of the data collected in this study are compiled in Table 1, on the following page. Although we were not able to successfully probe the binding site environment with tethered agonists, all hope is not lost. A few lines of inquiry are still available to us, among them:

We can coexpress 5HT_{3A}(13'S)Rs with 5HT_{3A}(183TAG)Rs bearing TyrO2Q. Although coexpressing with the B subunit did not give constitutive activity-free receptors, this strategy may. It is possible that the number of wild type B subunits necessary to suppress spontaneous constitutive activity makes the channel poorly responsive to 5-HT (i.e. the 2:1 ratio).

We can coexpress 5HT_{3A}(9'T)Rs with 5HT_{3A}(183TAG)Rs bearing TyrO2Q. Expression levels of homopentameric 5HT_{3A}(183TAG, 9'T)Rs were undetectably low, but having fewer Ser mutations may help to increase expression.

Given the sequence and functional similarity of the binding sites of the 5HT₃R and the nAChR, it would be very interesting to compare the local pK_a of these two receptors. Since the 5HT₃R gates in response to a primary amine (5-HT) rather than a quaternary ammonium like ACh, it may have an unperturbed binding site pK_a. It would have evolved to stabilize its endogenous agonist in its binding site in an active state, which would require stabilizing it as a protonated, cationic entity. If this could happen in the face of such sequence similarity to the muscle nAChR, identifying the roots of such a difference could be quite valuable.

Table 1. Tethered Agonist Experiments with the 5HT₃R

Construct	aa183	I(5-HT) ^a	I(Block) ^b	I(pH 5.5) ^c	I(pH 6.5) ^c	I(pH 8.5) ^c	n ^d
5HT ₃ A-183TAG-13'S	Trp	- 500 nA	+ 75 nA	- 100 nA	- 30 nA	+ 10 nA	2
5HT ₃ A-183TAG-13'S	74mer	0 nA	+ 50 nA	+ 10 nA	0 nA	+ 50 nA	2
5HT ₃ A-183TAG-13'S	TyrO3Q	- 50 nA	+ 75 nA	- 75 nA	- 10 nA	- 25 nA	2
5HT ₃ A-183TAG-13'S	TyrO3P	- 100 nA	+ 100 nA	- 75 nA	- 10 nA	- 25 nA	2
5HT ₃ A-183TAG-9'T§	Trp	0 nA	0 nA	—	—	—	2X6
5HT ₃ A-183TAG-9'T§	TyrO3Q	0 nA	0 nA	—	—	—	2X6
5HT ₃ A-183TAG-9'T§	TyrO3P	0 nA	0 nA	—	—	—	2X6
5HT ₃ A-183TAG-13'S/B (2:1)	Trp	0 nA	0 nA	—	—	—	3
5HT ₃ A-183TAG-13'S/B (5:1)	Trp	- 150 nA	+ 50 nA*	—	—	—	3
5HT ₃ A-183TAG-13'S/B (10:1)	Trp	- 500 nA	+ 50 nA*	—	—	—	3
5HT ₃ A-183TAG-13'S/B (2:1)	TyrO3Q	0 nA	0 nA	—	—	—	3X3
5HT ₃ A-183TAG-13'S/B (5:1)	TyrO3Q	0 nA	0 nA	—	—	—	3X3
5HT ₃ A-183TAG-13'S/B (10:1)	TyrO3Q	0 nA	0 nA	—	—	—	3X3
5HT ₃ A-183TAG-13'S/B (10:1)	TyrO2Q	- 25 nA‡	+ 300 nA	—	—	—	5
5HT ₃ A-183TAG-13'S/B (10:1)	TyrO4Q	0 nA	+ 40 nA	—	—	—	3
5HT ₃ A-183TAG-13'S/B (10:1)	TyrO5Q	0 nA	+ 20 nA	—	—	—	3
5HT ₃ A-183TAG	Trp	- 2500 nA	0 nA	—	—	—	3
5HT ₃ A-183TAG	TyrO2Q	0 nA	+ 20 nA	—	—	—	3
5HT ₃ A-183TAG	TyrO4Q	0 nA	0 nA	—	—	—	3

a I(5-HT) indicates response to 100 μ M 5-HT.

b I(Block) indicates response to 100 μ M TMB-8 or QX-314.

c I(pH X) indicates response to application of an agonist-free solution of pH X.

d n = Number of trials. AXB indicates B attempts on A days.

§ Remade mRNA twice. Agarose gel analysis indicated that it was the correct size. Sequencing analysis was confirmatory of the mutation.

* Some increased constitutive activity following agonist washout, as well as *de novo* constitutive activity.

‡ Large desensitization following inward current, almost as large as blocked current.

Materials and Methods

Unnatural amino suppression in *Xenopus* oocytes

The site-directed mutagenesis of the 5HT_{3A}R TAG mutants, gene construction and synthesis of suppressor tRNA and ligation of aminoacyl-dCA to tRNA have been described previously.^{2, 4} Analogous techniques were applied here to generate the 9' mutant in a plasmid containing the TAG 183 mutation. Plasmid DNAs were linearized with NotI, and mRNA was transcribed using the Ambion (Austin, TX) T7 mMESSAGE mMACHINE Kit.

Oocytes were removed from *Xenopus laevis* as described and maintained at 18 °C, in ND96 solution (96 mM NaCl/2 mM KCl/1.8 mM CaCl₂/1 mM MgCl₂/5 mM HEPES/2.5 mM sodium pyruvate/0.5 mM theophylline/10 g/ml Gentamycin, pH 7.5, with NaOH). Before microinjection, the NVOC-aminoacyl-tRNA was deprotected by irradiating the sample for 5 or 10 min. with a 1000 W Hg/Xe arc lamp (Oriel) operating at 400 W equipped with WG-335 and UG-11 filters (Schott). 4PO-protected tRNA-aa was mixed 1:1 with a solution of saturated I₂ in water and allowed to sit for ten minutes at room temperature. Each oocyte was injected with a 1:1 mixture of deprotected aminoacyl-tRNA (25-50 ng) and mRNA (12.5–18 ng of total at a concentration ratio of 20:1:1:1 for α:β:γ:δ subunits) in a volume of 50 nL.

Electrophysiological recordings

Voltage-clamped electrophysiological recordings were carried out 24-72 hours after injection. Whole-cell currents from oocytes were measured using a Geneclamp 500 amplifier and pCLAMP software (Axon Instruments, Foster City, CA) in the two-electrode voltage-clamp configuration. Microelectrodes were filled with 3 M KCl and had resistances ranging from 1.0 to 2.5 MΩ. Oocytes were continuously perfused with a nominally Ca²⁺-free bath solution consisting of 96 mM NaCl, 2 mM KCl, 1 mM MgCl₂, and 5 mM HEPES (pH 7.5). Microscopic 5-HT-induced and TMB-8 or QX-314-blocked currents were recorded in response to bath application of 5-HT and TMB-8 at a holding potential of -80 mV. Low (5.5 - 6.5) and high (8.5 and 9.0) pH solutions were of the same composition as Ca²⁺-free bath with MES (low) or CHES (high) substituted for HEPES buffer. To ensure that changes in buffer were not responsible for the observed changes in channel conductance, recordings were taken at pH 7.0 and 8.0 in HEPES alongside recordings in MES and CHES.

References

- (1) Reeves, D. C.; Lummis, S. C. R., *Mol. Memb. Biol.* **2002**, 19, 11-26 Maricq, A. V.; Peterson, A. S.; Brake, A. J.; Myers, R. M.; Julius, D., *Science* **1991**, 254, 432-437.
- (2) Beene, D. L.; Brandt, G. S.; Zhong, W.; Zacharias, N. M.; Lester, H. A.; Dougherty, D. A., *Biochem.* **2002**, 41, 10262-10269.
- (3) Reeves, D. C.; Sayed, M. R. F.; Chau, P. L.; Price, K. L.; Lummis, S. C. R., *Biophys. J.* **2003**, 84, 2338-2344.
- (4) Dang, H.; England, P. M.; Farivar, S. S.; Dougherty, D. A.; Lester, H. A., *Mol. Pharmacol.* **2000**, 57, 1114-1122.
- (5) Labarca, C. G.; Nowak, M. W.; Zhang, Y.; Tang, L.; Deshpande, P.; Lester, H. A., *Nature* **1995**, 376, 514-516.
- (6) Li, L.; Zhong, W.; Zacharias, N.; Gibbs, C.; Lester, H. A.; Dougherty, D. A., *Chem. Biol.* **2001**, 8, 47-58.